J. W. Jewel

NATIONAL ADVISORY COMMITTEE FOR AERONAUTICS

WARTIME REPORT

ORIGINALLY ISSUED
May 1942 as
Advance Restricted Report

EFFECT OF INLET-AIR VELOCITY DISTRIBUTION ON THE METERING PRESSURE OF AN INJECTION-TYPE AIRCRAFT CARBURETOR

By George F. Kinghorn

Langley Memorial Aeronautical Laboratory
Langley Field, Va.

NACA

WASHINGTON

NATIONAL ADVISORY COMMITTEE FOR AERONAUTICS

ADVANCE RESTRICTED REPORT

EFFECT OF INLET-AIR VELOCITY DISTRIBUTION ON THE METERING PRESSURE OF AN INJECTION-TYPE AIRCRAFT CARBURETOR

By George F. Kinghorn

SUMMARY

Tests have been made of a three-barrel pressure carburetor to determine the effect of nonuniformity of the air flow in the intake duct upon the metering of the carburetor. Measurements were made in the air side of the metering system and in the carburetor barrels for a large variety of flow distributions. For the most nonuniform air-flow distributions the metering pressure was found to be increased about 11 percent, which is equivalent to a 5-percent enriching of the mixture. The flow behind a square unvaned elbow was found to be more nonuniform than that behind a rounded unvaned elbow and led to an increase in the metering pressure several times as large as the increase due to the rounded elbow.

Certain features of the altitude compensation were also investigated. The results of these tests indicated that the altitude compensation was satisfactory over the limited range tested.

INTRODUCTION

Several recent installations of pressure-type carburetors on airplanes equipped with single-stage engines have encountered difficulties in maintaining in flight at altitude the fuel-air ratios indicated from results obtained in ground tests. Serious enrichment of the mixture has been reported when the engine operates in high-blower condition near the critical altitude. An understanding of the reasons for the malfunctioning of the carburetor has been of primary interest. Tests to determine these reasons have been the subject of several investigations. Two such investigations are reported in references 1 and 2.

The discrepancies between the characteristics of the carburetor in flight and those predicted from test-stand and air-box calibration led to a study of the differences in the operating conditions. On the test stand the air-inlet scoops are designed to provide a uniform velocity distribution to the metering elements of the carburetor; whereas, in flight the existence of the friction boundary layer, the propeller slipstream, and the interference of adjacent airplane elements sometimes leads to extreme dissymmetry in the velocity-distribution pattern ahead of the carburetor venturis. Since in other respects the ground tests appeared to reproduce flight conditions, an investigation was begun to determine the effect on the metering of nonuniform distribution of air flow to the carburetor. A three-barrel pressure-type carburetor was mounted on the intake of a blower tunnel and the metering was measured for a wide range of artificially established, nonuniform inlet flow distributions.

The effect of the throttle position on the metering and the operation of the altitude compensating device were also investigated to a limited extent. The effect of the nonuniformity of the air flow at the carburetor on the air flow at the supercharger inlet and the resultant mixture distribution to the cylinders was not determined.

SYMBOLS

q	dynamic pressure
q_{av}	dynamic pressure corresponding to average velocity
p	static pressure
A-B	metering pressure
Δ(A-B)	difference in metering pressure from that obtained with a uniform velocity distribution for the same mass flow
Δp_V	total pressure of air entering boost venturi minus static pressure at outlet

ΔH loss in total pressure between carburetor inlet and throat of main venturi

ρ air density

APPARATUS AND METHODS

A Stromberg PT-13F1 carburetor was used for the tests. A diagram of the carburetor is given in figure 1. The suction at the throat of the boost venturi is transmitted to chamber B and the pressure on the impact tubes is transmitted to chamber A. For a given air density, the differential pressure (A-B) will have a single value for each mass flow of air. In order to insure that this value will be the same for each mass flow, regardless of the air density, a fixed orifice is introduced between chambers A and B, and a variable orifice (automatic mixture control unit) is introduced between the impact tubes and chamber A. As the air density decreases, the automatic mixture control unit valve lowers, further restricting the air passage to chamber A. The pressure in chamber A is thus reduced maintaining the pressure across the air diaphragm (A-B) at the desired value.

For each mass flow of air, as indicated by A-B, the carburetor is arranged to supply the proper amount of fuel. The force on the air diaphragm is transmitted by a connecting rod to the fuel diaphragm, which develops a differential pressure across the fuel-metering jets and thus controls the flow of fuel regardless of the entering fuel pressure. As the flow of fuel varies with the square root of the pressure difference across the fuel and air diaphragms, a measurement of the metering pressure (A-B) is indicative of the mass of fuel flowing to the engine.

The carburetor was installed in a tunnel (fig. 2) with an axial-flow fan behind the carburetor to draw the air through with a minimum of turbulence and fluctuation caused by the fan. In order to lower the air resistance of the carburetor, the butterfly valves were removed, the sides of the barrels were faired below the throats of the main venturis, and the adapter between carburetor and diffuser was designed to give a slow expansion from each of the three barrels into the diffuser. Later, the fairings were removed and the butterfly valves were installed to determine their effect upon the variations in metering

pressure. A bell, followed by a straight, constant-area duct 18 inches long, was placed in front of the carburetor. A large part of the testing consisted in pressure measurements for different distributions of the air velocity in the duct just ahead of the carburetor. The measurements were made in the air side of the metering system, that is, in chambers A and B; in the reservoir connecting the total head tubes; and in the throat and the outlet of the boost venturi. The velocity distribution for most of the tests was varied by introducing screens of different mesh or baffles of different spacing at the beginning of the straight section of the entrance duct, 18 inches from the carburetor flange. In others, 90° elbows were introduced between the bell and the carburetor. A sharp-cornered unvaned elbow and a rounded unvaned elbow were used (fig. 3).

The velocity and pressure distributions were found from measurements made with small total-pressure and static-pressure tubes. These measurements were made in a plane 4.5 inches ahead of the carburetor flange. The measurements to determine the air-flow quantity were made with small total-pressure and static-pressure tubes in the bell 10 inches in front of the straight section and were checked by measurements in an orifice plate in the diffuser. The air-flow quantity used in most of the tests was approximately 10,000 pounds per hour and the air density was 0.00238 slug per cubic foot.

Tests were also made to check certain features of the altitude compensation. In these tests the pressure inside the altitude compensator was reduced to simulate altitude conditions. The pressure throughout the carburetor except in the compensator itself was allowed to remain at its normal sea-level value. The effects of variations in temperature were not investigated. In all the above-mentioned tests the mixture control was set at automatic rich. Some additional tests were made with the setting at emergency rich.

RESULTS

The dynamic-pressure distribution for the unobstructed inlet is shown in figure 4. The data obtained from the tests in which screens and baffles were used to create various velocity and pressure distributions in the duct

ahead of the carburetor are shown in figures 5 to 13. The results of the tests in which the velocity variations were created by the introduction of an elbow in the duct leading to the carburetor are shown in figures 14 to 22. Each figure shows the variations in dynamic pressure across the small dimension of the duct in the plane of measurement. (See fig. 2.) The static pressure is also plotted in cases where it is not uniform across the carburetor face. The static pressure is referred to the pressure of the air outside the duct. Both these pressures are given in terms of the dynamic pressure corresponding to the average velocity in the straight section of the duct. In each of the figures the change in metering pressure from that measured for a uniform velocity distribution (fig. 4) is given. In most cases, the ratio of the metering pressure to the pressure drop measured across the boost venturi, $(A-B)/\Delta p_v$, is also given. Tests were made with the same velocity distribution at several different air quantities but, as these results showed that with the same distribution the metering pressure is proportional to the square of the mass flow (at the same air density), the results have been reduced to a nondimensional form.

In all the tests, the pressure in the reservoir connecting to the total-pressure tubes never differed from the static pressure in the duct by more than 2 percent of the metering pressure.

The results obtained with the throttled valve installed showed that, for any constant throttle position, the variations in metering pressure with different velocity and pressure distributions were substantially the same as the variations measured without the throttle valves in place. The metering pressure seems to be a function of the throttle position and, for all the different velocity distributions tested, the metering pressure at full throttle was about 3 percent less than with the throttle valves removed. At a throttle position halfway between full-open and full-closed the metering pressure was reduced another 3.5 percent.

Additional data obtained with a uniform flow across the carburetor are presented in figure 23. The average loss in total pressure at the throat of the main venturi is about 8 percent of the static-pressure drop at the throat. The variation of the metering pressure with the square of the mass flow, for a uniform pressure distribution, is given in figures 24 and 25 with the mixture control set at automatic rich and emergency rich.

Results of the tests on the altitude compensator are shown in figure 26. Tests with different pressures on the compensator were generally run at different air quantities and the results were normalized, assuming that the straight-line function found between metering pressure and the square of the quantity held for all air densities. The required proportionality between metering pressure and the density ρ is shown by the dashed line; the points are experimental.

DISCUSSION

The results show that the metering pressure may be increased about 11 percent by nonuniformity of the flow in the duct ahead of the carburetor, corresponding to a 5-percent enrichment of the mixture. In the examination of the results, the following analysis has been found useful although it does not permit an exact correlation between the flow patterns and the measured increases in metering pressure.

For a given density, the metering pressure is determined by the difference between the average total pressure at the impact tubes and the static pressure at the throat of the boost venturi. In the idealized case, with uniform flow at the inlet, this difference is simply the dynamic pressure at the throat of the boost venturi. It will be convenient, however, to consider it in two parts:

(a) The difference between the average total pressure at the impact tubes and the static pressure at the throat of the main venturi

(b) The difference between the static pressure at the throat of the main venturi (where the outlet of the boost venturi is located) and the static pressure at the throat of the boost venturi

With a given mass flow, part (a) will be affected in two opposite ways by nonuniformity. First, considerations based on Bernoulli's equation alone indicate a reduction. Thus in a limiting case, if some of the impact tubes are in a dead-air space, they will read only the static pressure of this region and thus lower the indicated average total pressure. Actually, calculations

based on the observed velocity distributions in the inlet duct have shown that this reduction can be, at most, only a few percent of part (a). Second, considerations of the drag losses between the plane of the impact tubes and the throat of the main venturi indicate an increase with nonuniform flow. The region around and just back of the impact tubes contains many obstructions, such as the impact tubes themselves, the boost venturi, and the arms that support the boost venturi. From figure 23, which shows a total-pressure survey across the throat of the main venturi, it is estimated that the obstructions occasion a loss in static pressure of about 8 percent of part (a) for uniform flow. For nonuniform flow, the higher losses in the high-velocity air should cause a net increase in this value, with a corresponding increase in the difference between the average impact pressure and the static pressure at the throat. In general, this second effect appears to somewhat exceed the first in magnitude.

Part (b), which is several times as much as part (a), should be determined by the velocity of the air through the boost venturi which, in turn, should be determined by the difference Δp_V between the total pressure at its inlet and the static pressure at its outlet. It was expected that the observed variations in metering pressure would be directly reflected in variations of Δp_V. Measurements, however, showed that, for a given mass flow, Δp_V was practically constant for a widely different inlet-velocity distribution. This result indicates that the velocity through the boost venturi is not uniquely determined by Δp_V but may, with poor flow in the duct, be increased as much as 5 percent over that with uniform flow in the duct for a given Δp_V. The explanation possibly lies in the increased turbulence associated with the poorer flow, which may cause the flow in the expanding part of the boost venturi to adhere to the wall where it would otherwise separate. Calculations indicate that the laminar boundary layer on the inner wall of the boost venturi should be on the verge of separation about 1 inch from the throat and that, furthermore, the Reynolds number of the boundary layer at this point is in the critical range. Some slight turbulence in the flow might thus suffice to cause transition to a turbulent boundary layer; whereas, in perfectly smooth flow, the boundary layer might simply separate from the wall. Careful measurements of the flow inside the boost venturi might add

information on the subject. It may be that a deliberate disturbance of the flow, such as might be effected by putting a slight ridge near the throat of the boost venturi, would insure transition to the turbulent type of boundary layer in every case and cause the velocity through the boost venturi to be more nearly determined by Δp_v alone.

The altitude compensation appears to be fairly good over the limited range tested. The tests showed compensation to within 3 percent, which is of the same order as the accuracy of the tests.

The effect of the throttle on the metering characteristics may be ascribed to the distortion of the field of flow in the throat of the main venturi by the presence of the throttle valve. The valve causes a relative reduction in velocity (increase in pressure) near the middle and thereby reduces the flow through the boost venturi.

Figures 14 to 22 are of incidental interest with regard to the flow of air around square and rounded bends. Thus, figures 22, 21, and 20 show, respectively, the velocity distribution near the far side of the rounded bend, the separation of the flow from the inner wall in the subsequent deceleration, and the low-energy flow along the inner wall that results from the separation. Figures 15 and 16 (or 18 and 19) show the complete separation of the flow from the inner side of the square bend and the crowding of the flow into the outer half of the channel as far as 8 inches beyond the bend; figure 14 (or 17) shows that even 15 inches beyond the bend most of the flow is still in the outer part of the channel. It is interesting to note here that the main part of the energy loss occurs between 8 and 15 inches from the bend; that is, the loss does not occur directly at the separation but only in the subsequent churning. The energy loss is here proportional to $\int \sqrt{q}\ \Delta R ds$, where ΔR is the numerical difference between the static and the dynamic pressures indicated on the curves and s is the distance across the duct.

CONCLUSIONS

1. Carburetor metering pressures may be increased about 11 percent by extreme nonuniformity of the flow in the inlet duct. This increment in metering pressure corresponds to a 5-percent increase in mixture richness. The metering is not greatly affected by small deviations from uniform velocity distribution at the carburetor flange.

2. The difference between the total pressure at the inlet of the boost venturi and the static pressure at the outlet is nearly constant for a wide variety of flow conditions in the inlet.

3. The nonuniform velocity distribution behind the square unvaned elbow that was tested led to increases in the carburetor metering pressure several times larger than the increases due to a rounded elbow.

Langley Memorial Aeronautical Laboratory,
National Advisory Committee for Aeronautics,
Langley Field, Va.

REFERENCES

1. Mock, Frank C.: Aircraft Carburetor Airscoops and Their Effect on Fuel-Air Metering in Flight. SAE Jour., vol. 50, no. 3, March 1942, pp. 102-119.

2. Kittler, M. J.: Design of Airscoops for Aircraft Carburetors. SAE Jour., vol. 49, no. 5, Nov. 1941, pp. 501-508.

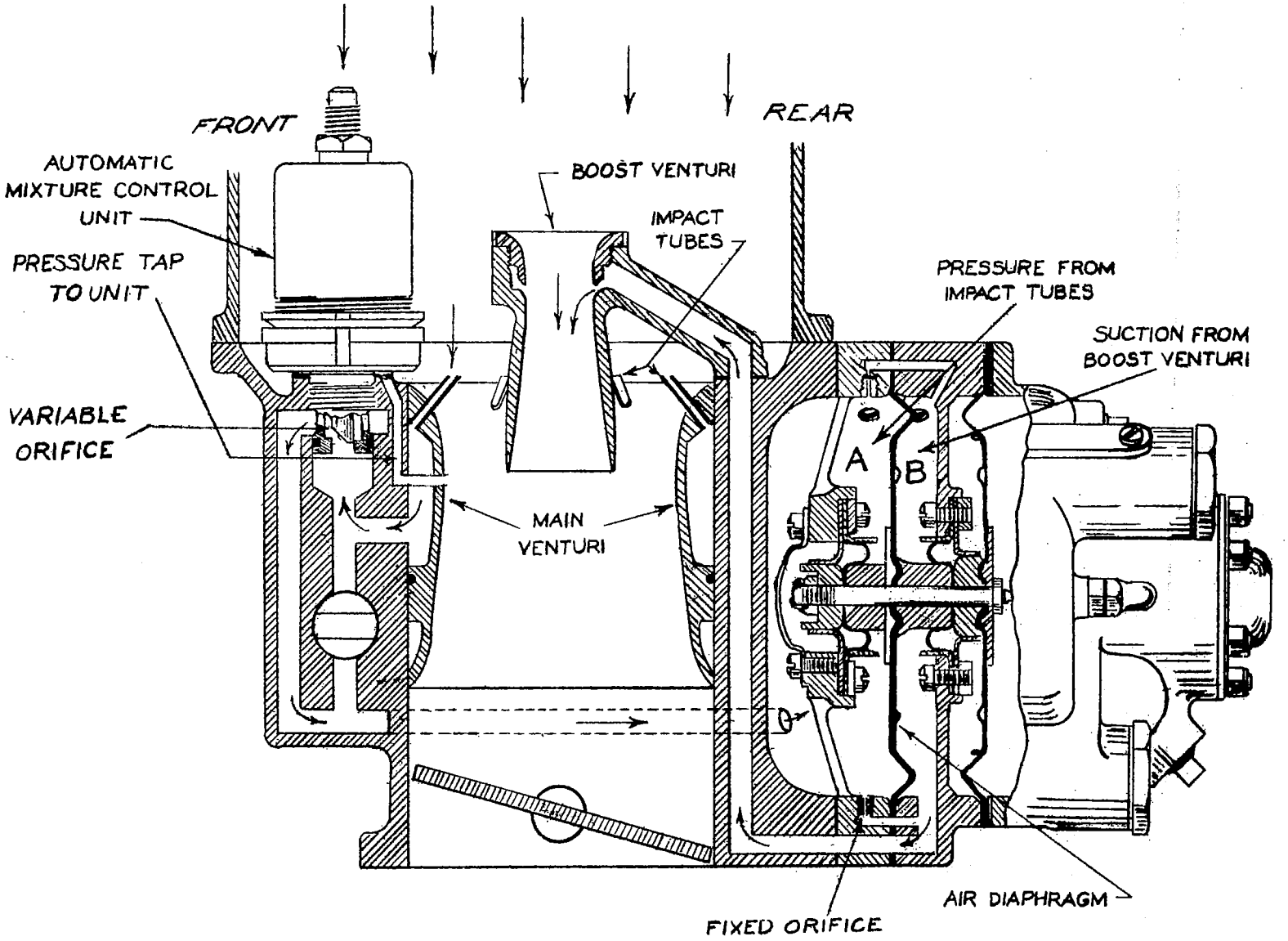

Figure 1.- Section through carburetor.

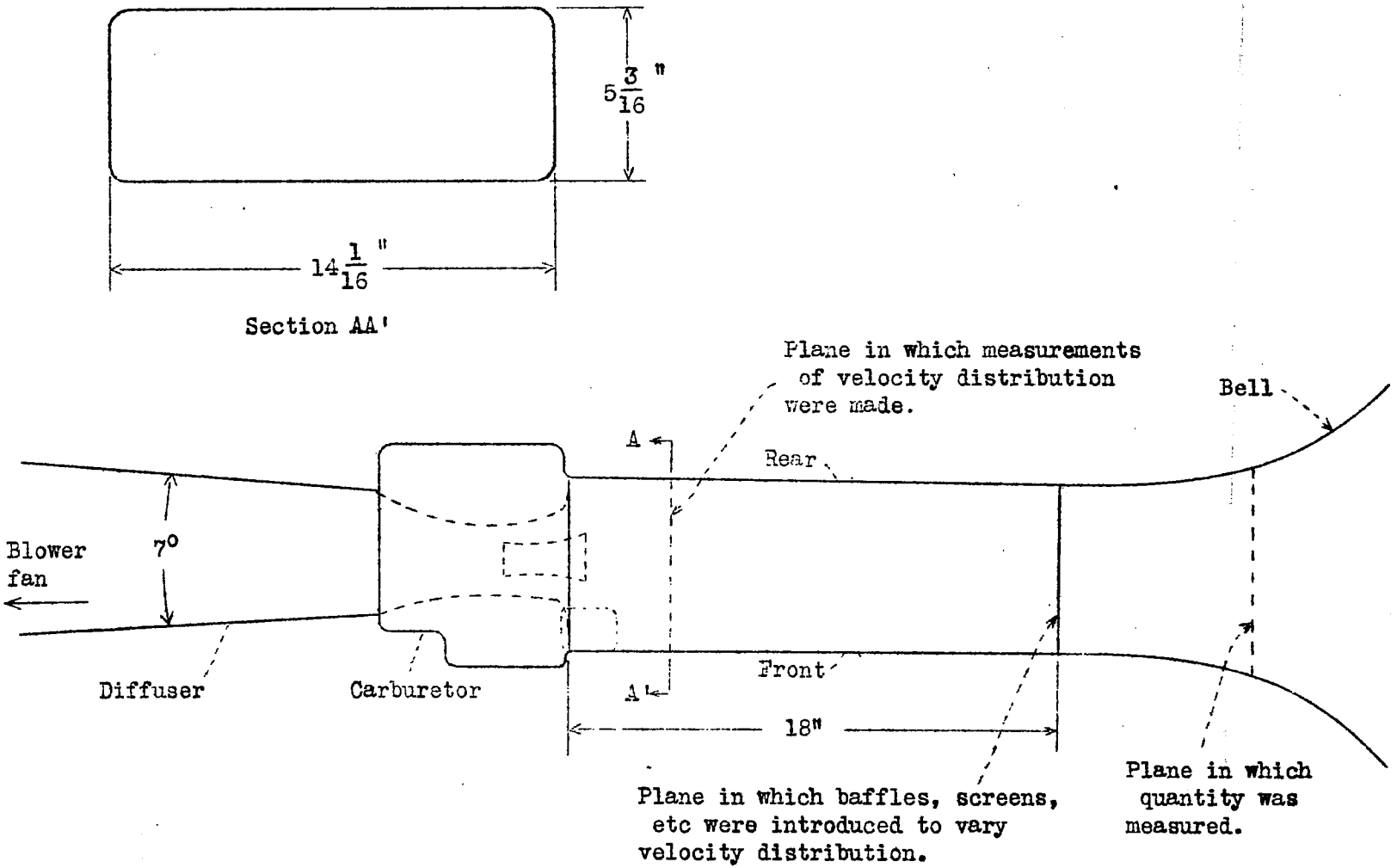

Figure 2.- Test set-up.

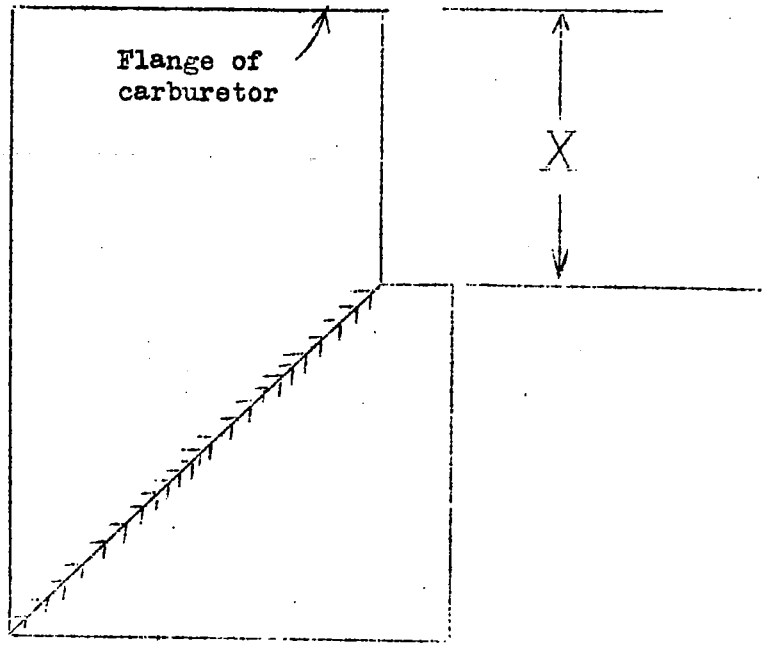

(a) Square elbow.

Figure 3.- Sections of square and round elbows. X is the distance from the carburetor.

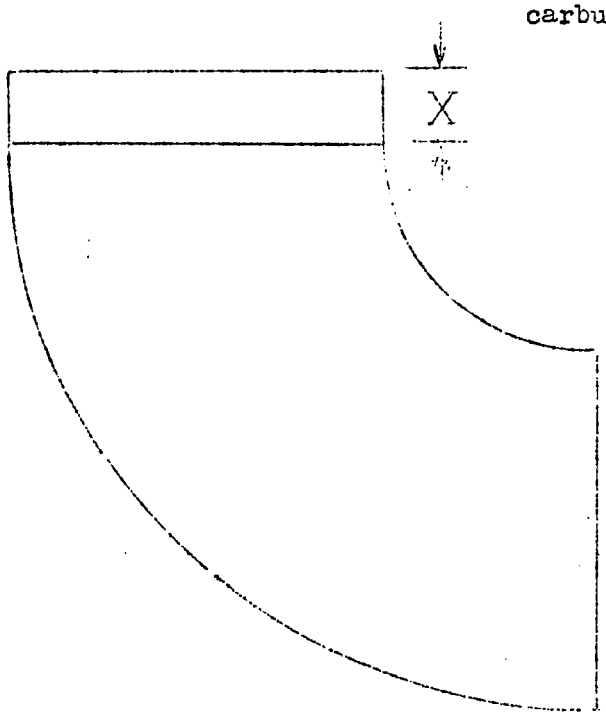

(b) Rounded elbow.

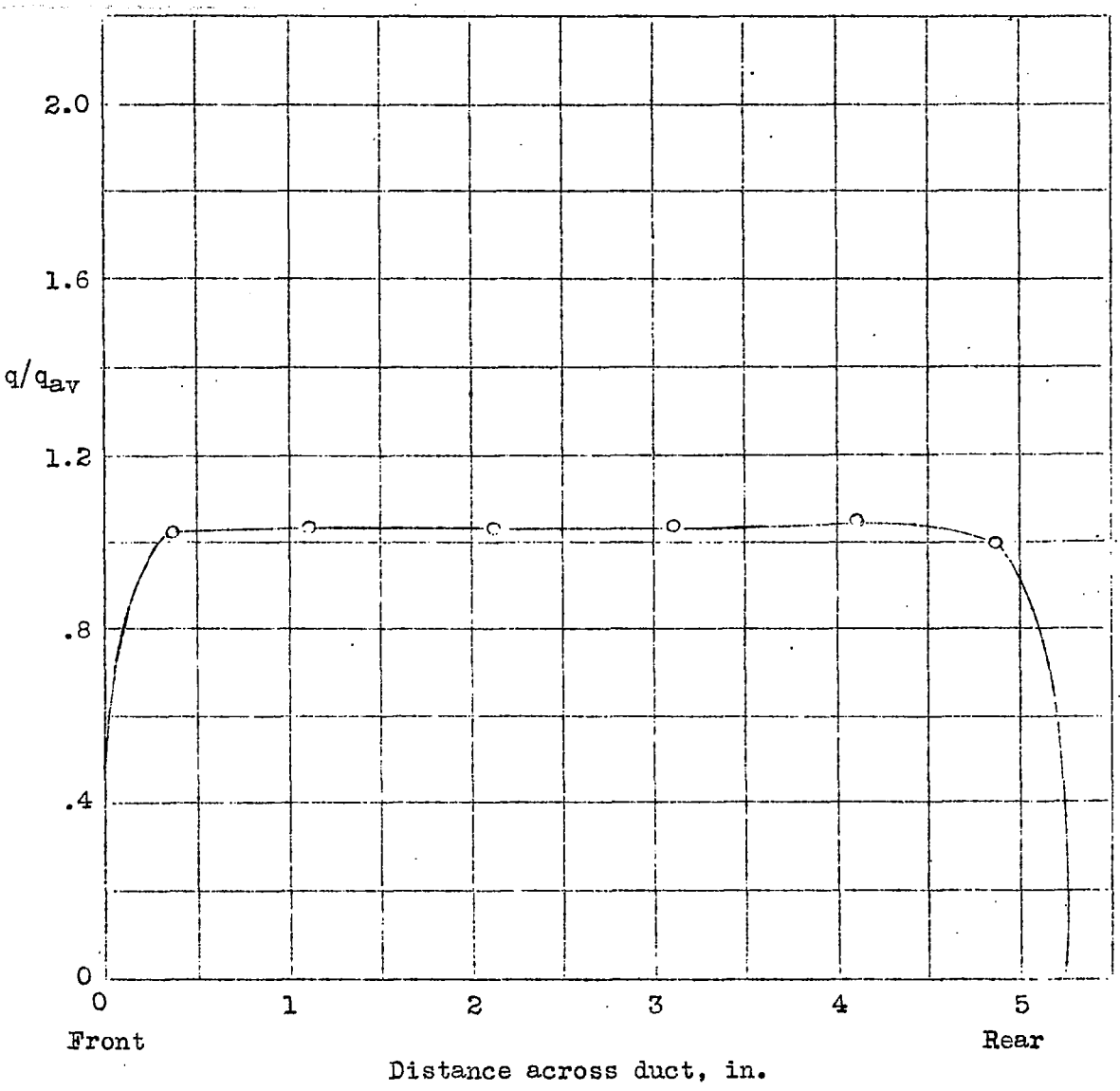

Figure 4.- Dynamic-pressure distribution used as a reference in comparing the metering pressures of the other distributions. $\frac{A-B}{\Delta p_V} = 2.63$.

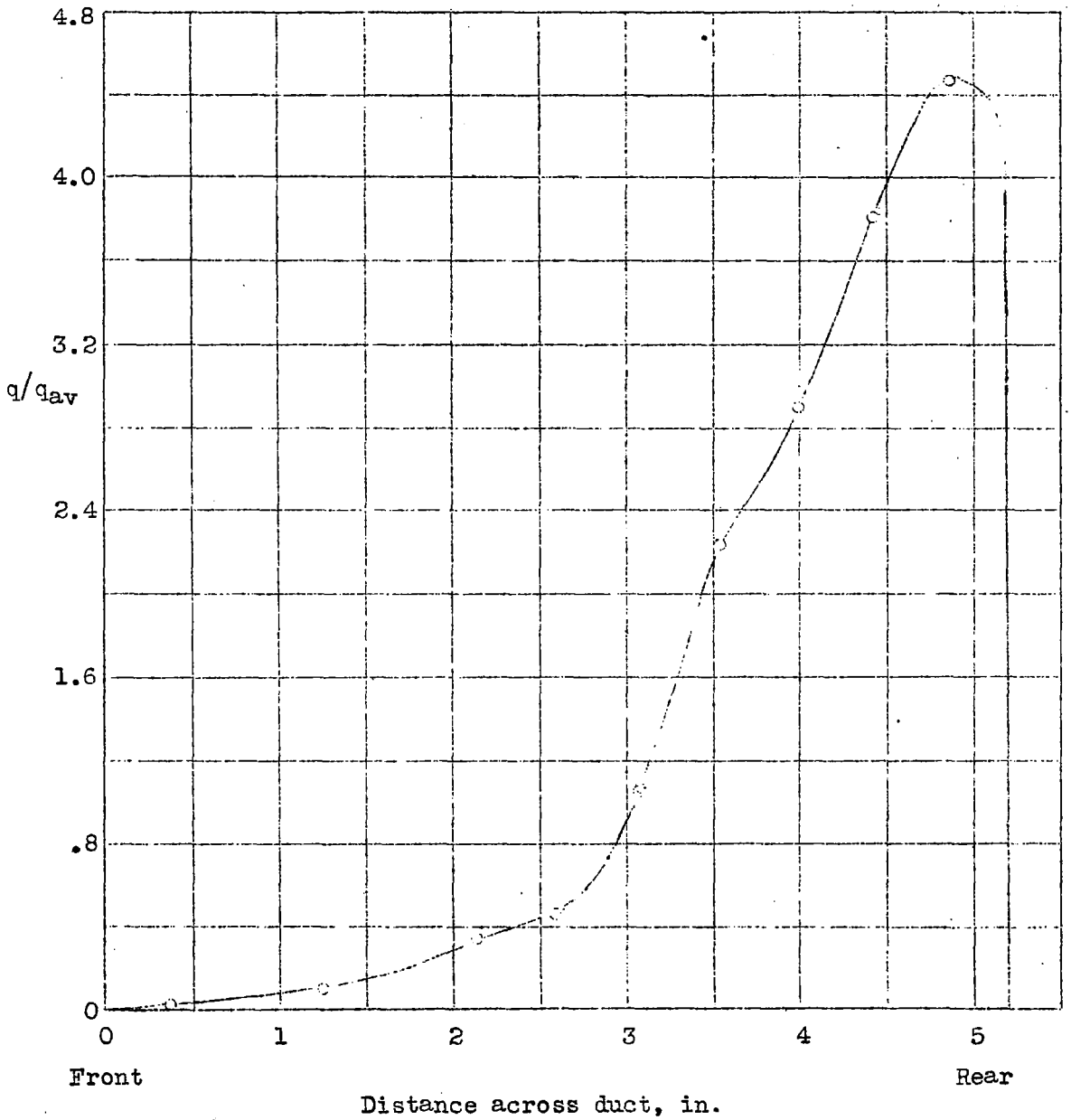

Figure 5.- Dynamic-pressure distribution in front of the carburetor and increment of metering pressure. Δ(A-B) = 7 percent.

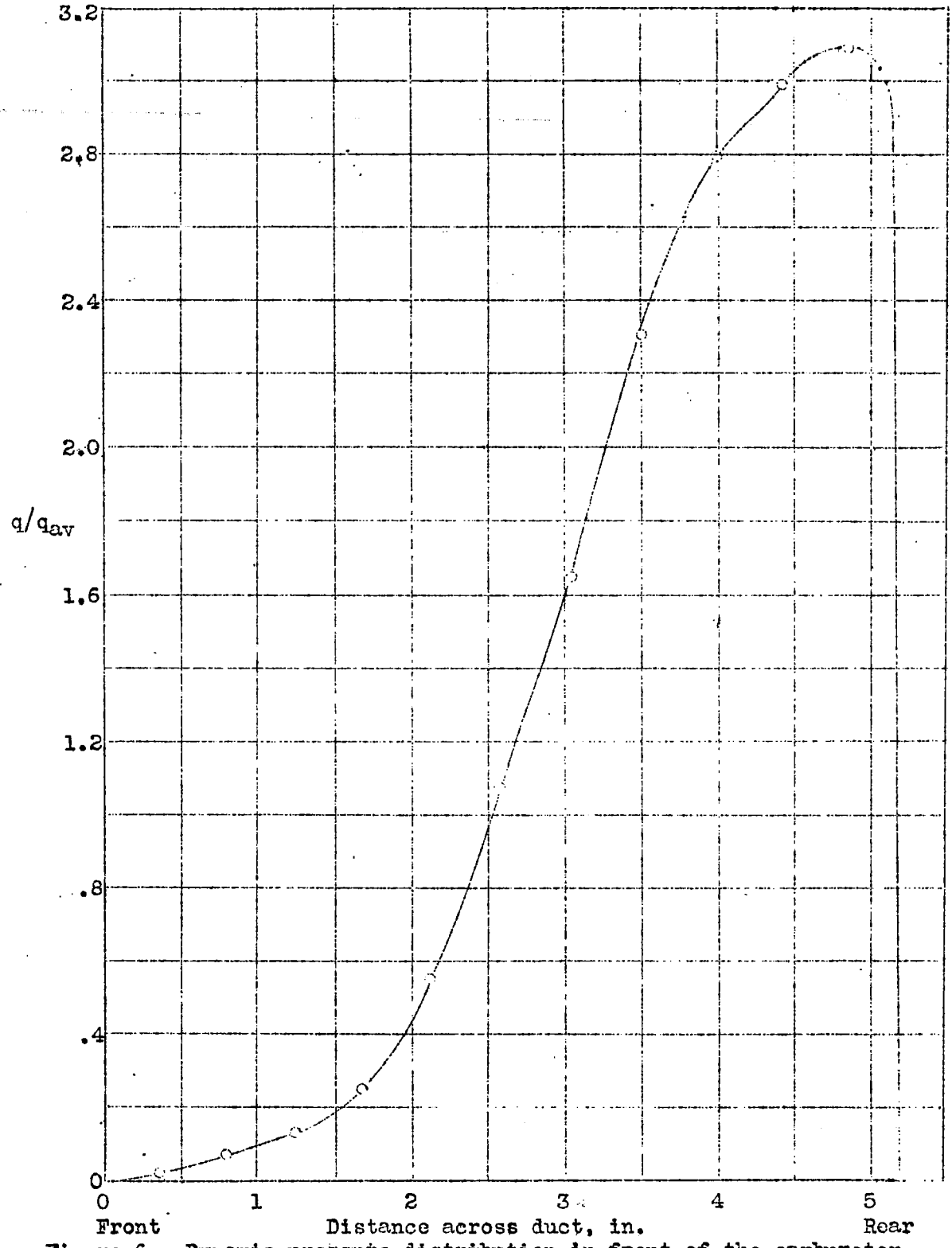

Figure 6.- Dynamic-pressure distribution in front of the carburetor and increment of metering pressure. Δ(A-B) = 6.5 percent.

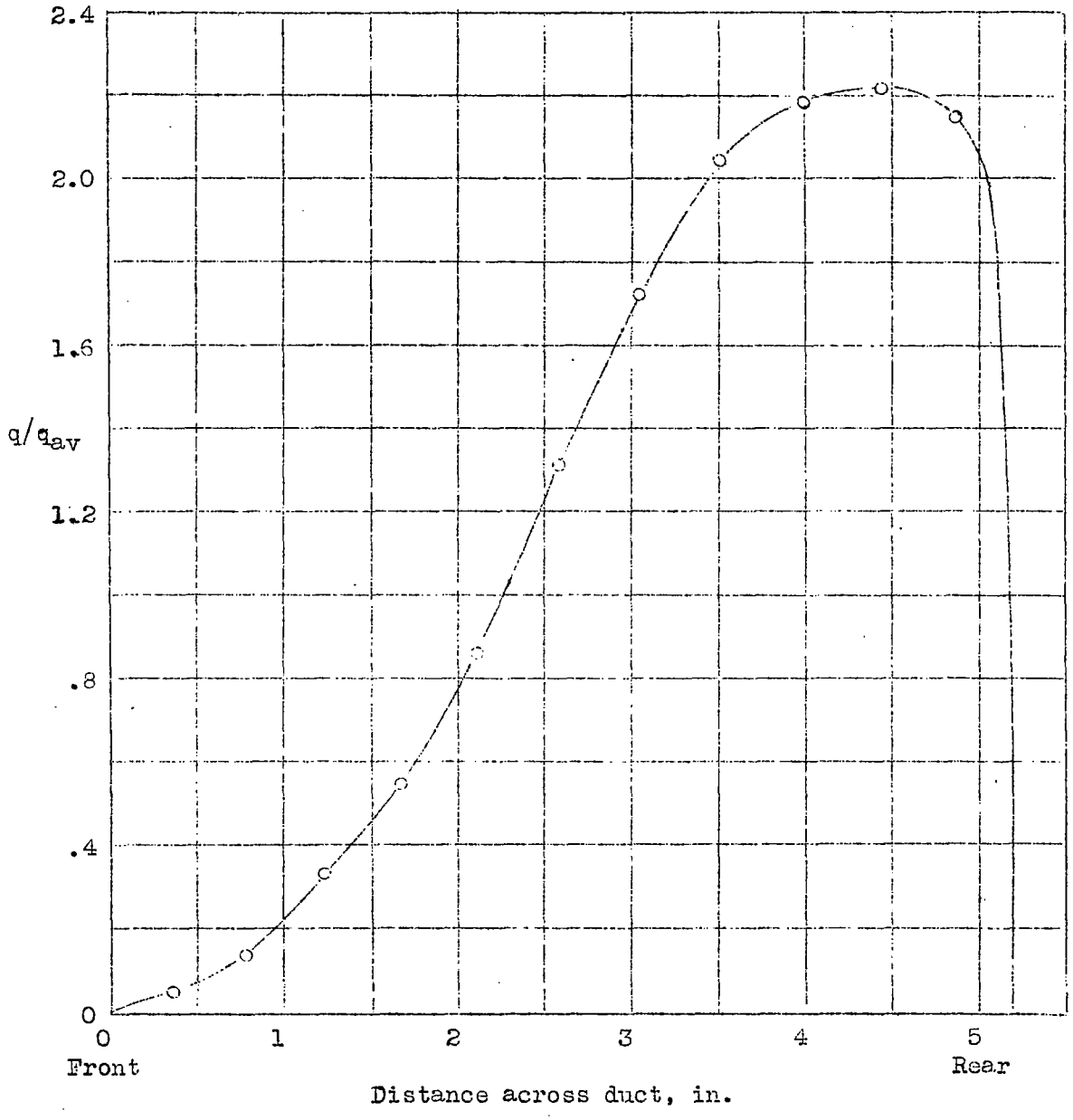

Figure 7.- Dynamic-pressure distribution in front of the carburetor and increment of metering pressure. Δ(A-B) = 3 percent.

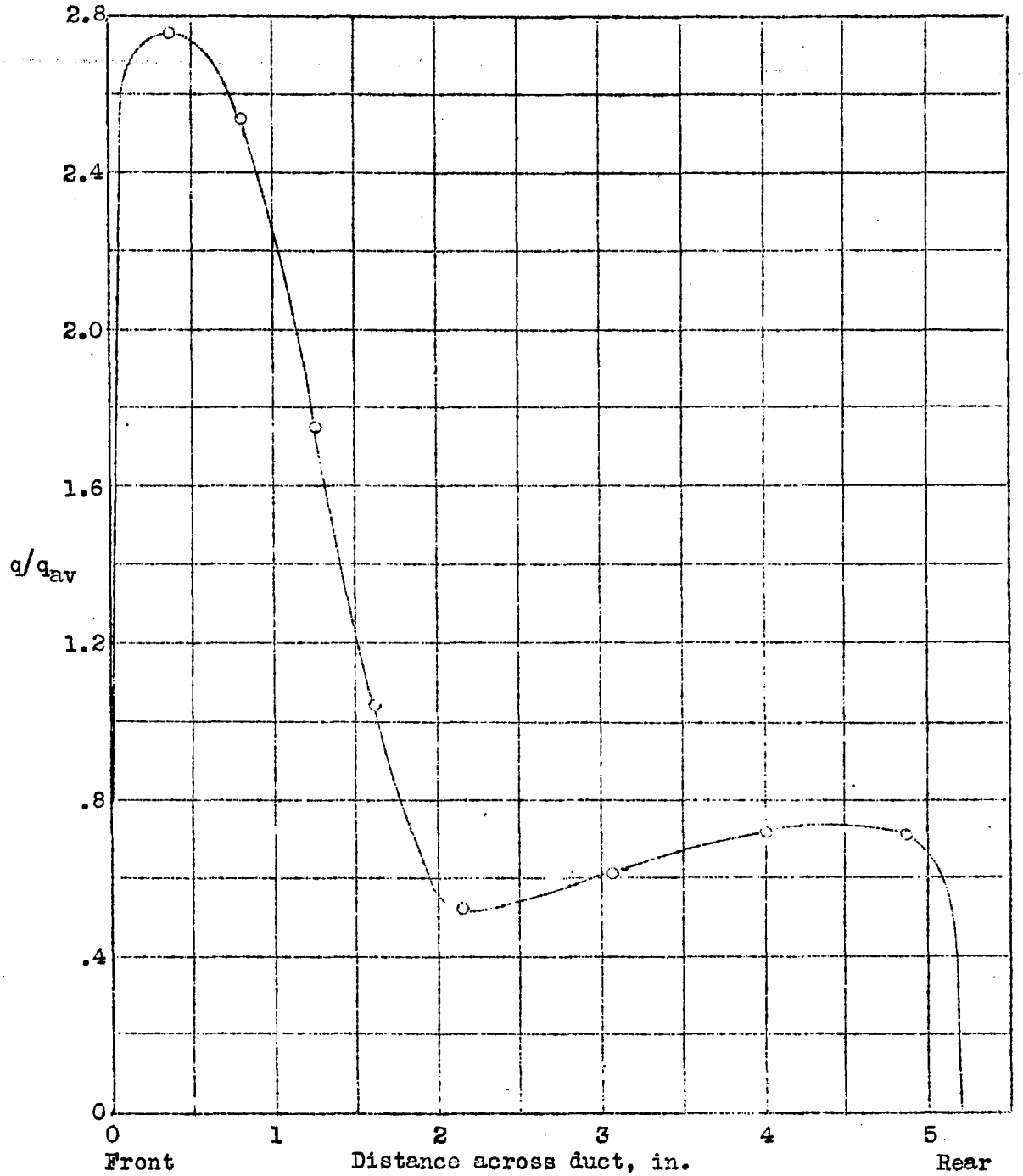

Figure 8.- Dynamic-pressure distribution in front of the carburetor and increment of metering pressure. Δ(A-B) = 5.5 percent.

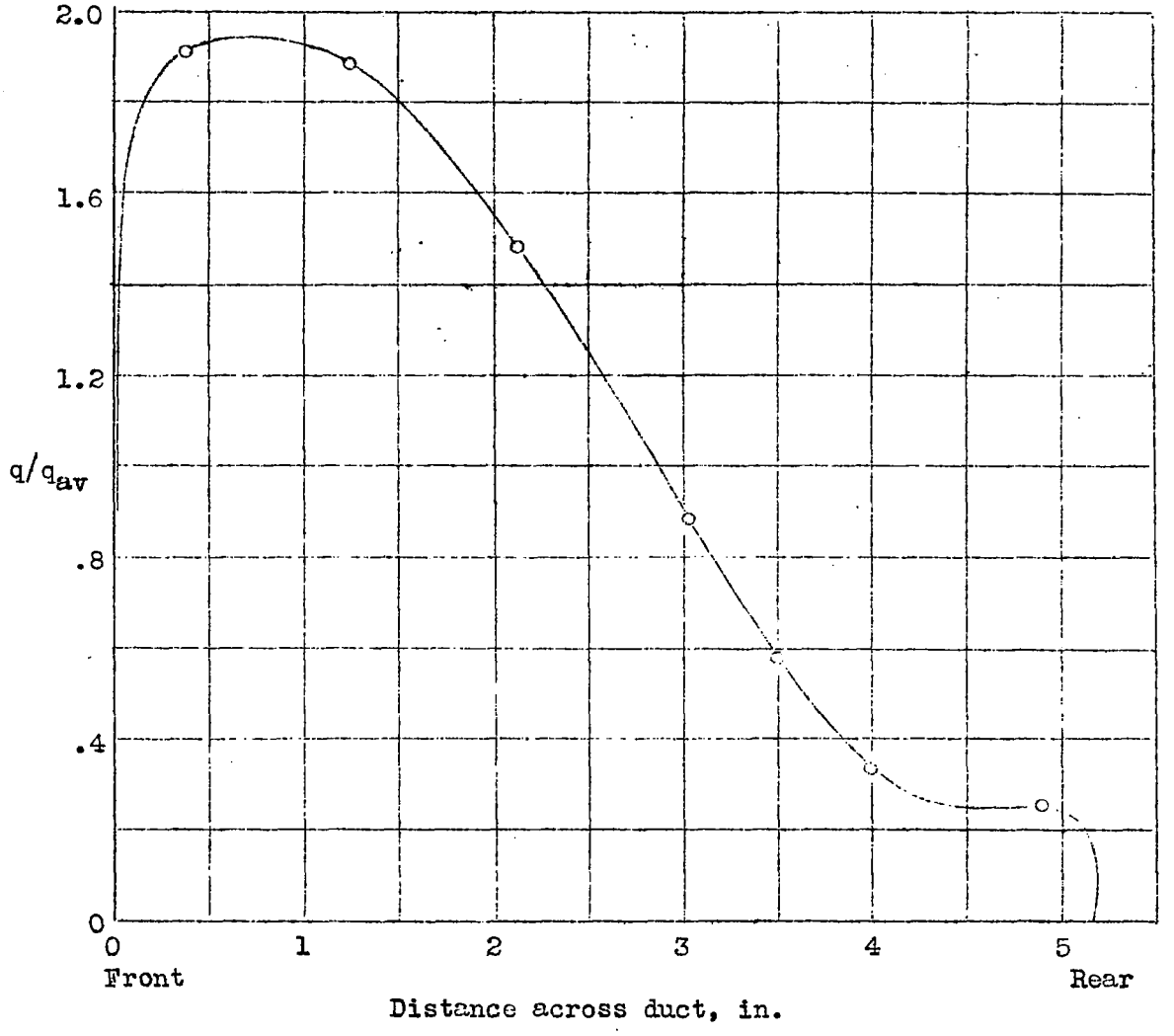

Figure 9.- Dynamic-pressure distribution in front of the carburetor and increment of metering pressure. $\Delta(A-B)$ = 8 percent.

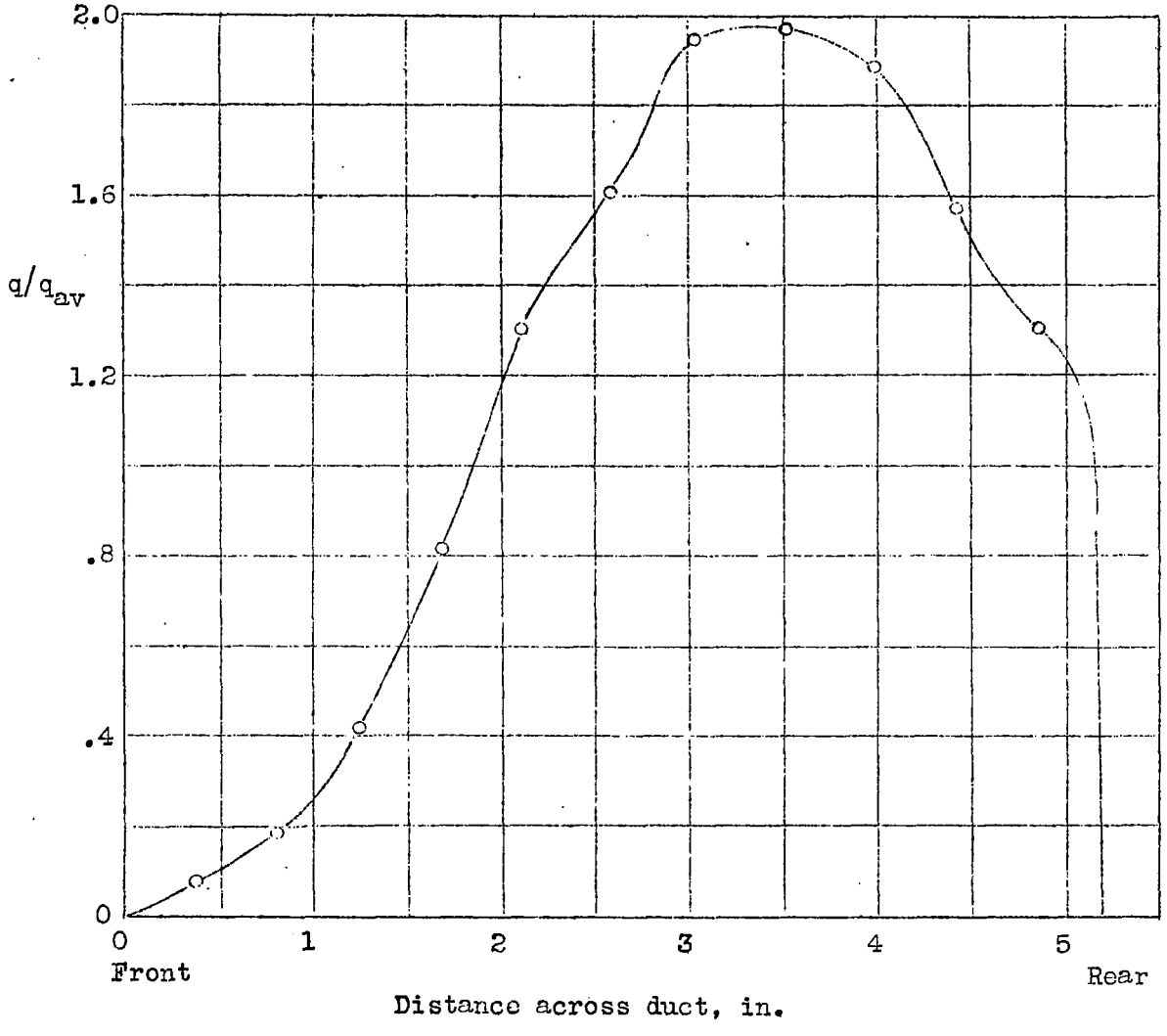

Figure 10.- Dynamic-pressure distribution in front of the carburetor and increment of metering pressure. $\Delta(A-B)$ = 8 percent.

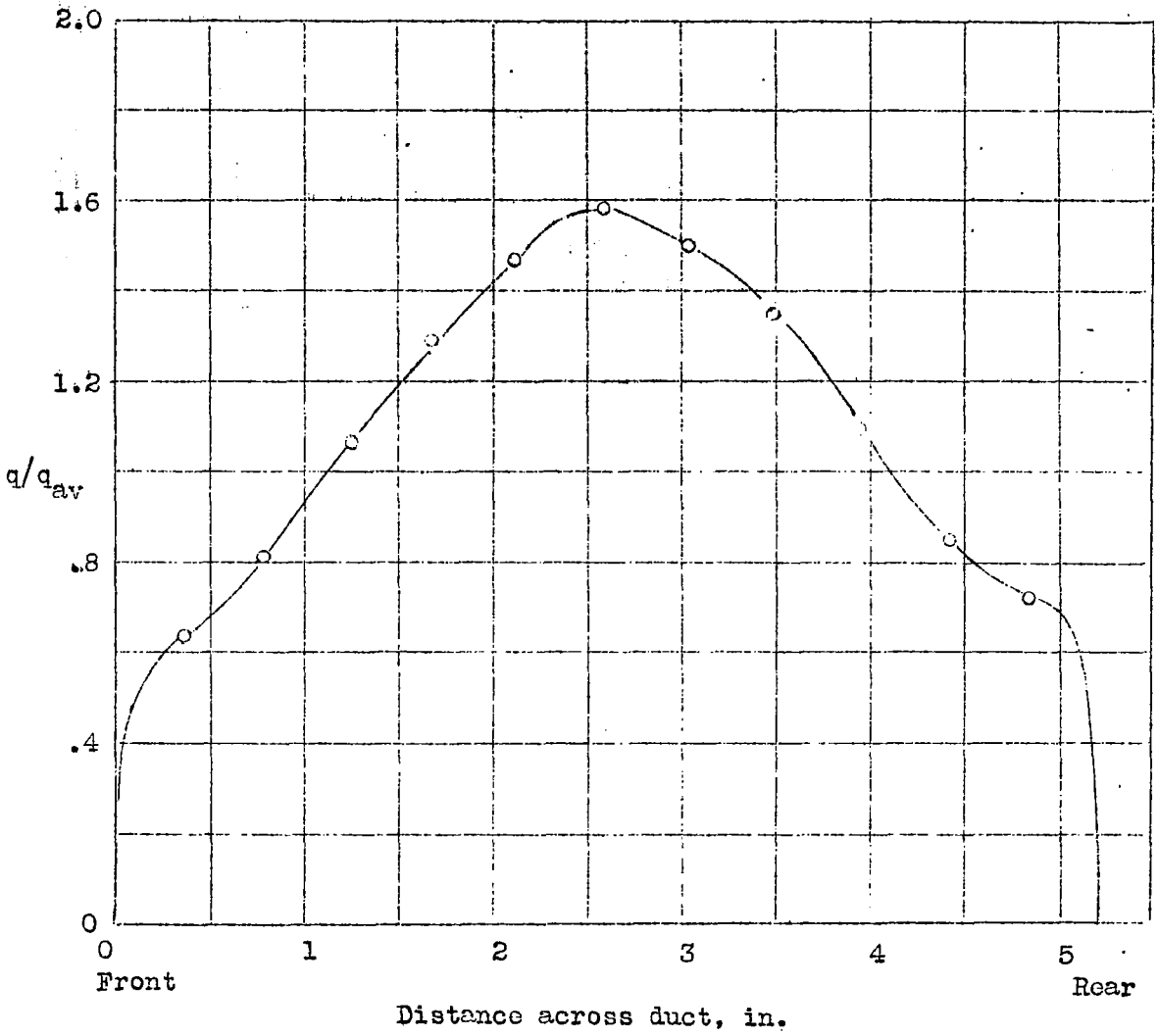

Figure 11.- Dynamic-pressure distribution in front of the carburetor and increment of metering pressure. $\Delta(A-B)$ = 3 percent.

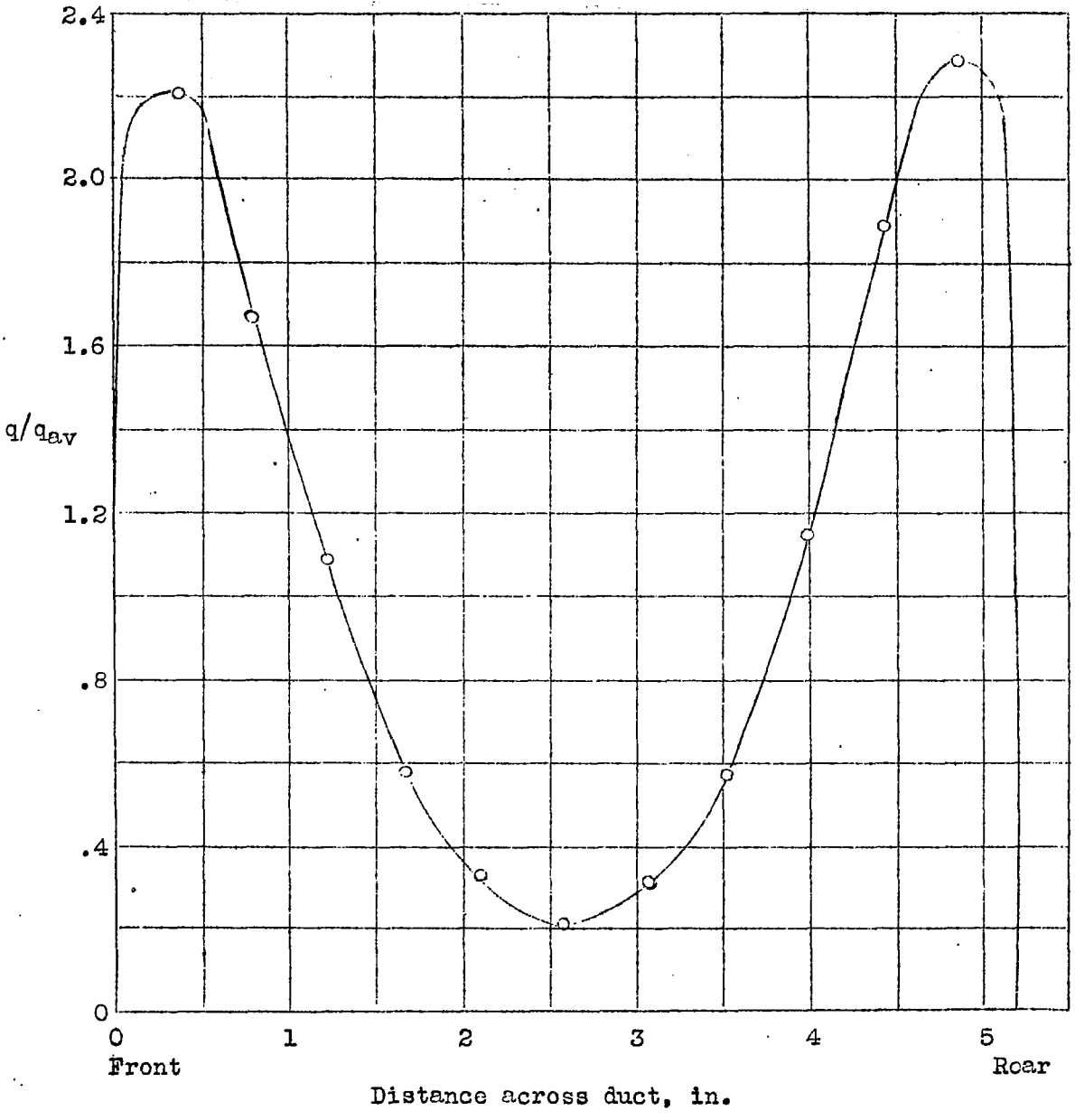

Figure 12.- Dynamic-pressure distribution in front of the carburetor and increment of metering pressure. $\Delta(A-B)$ = 5.5 percent.

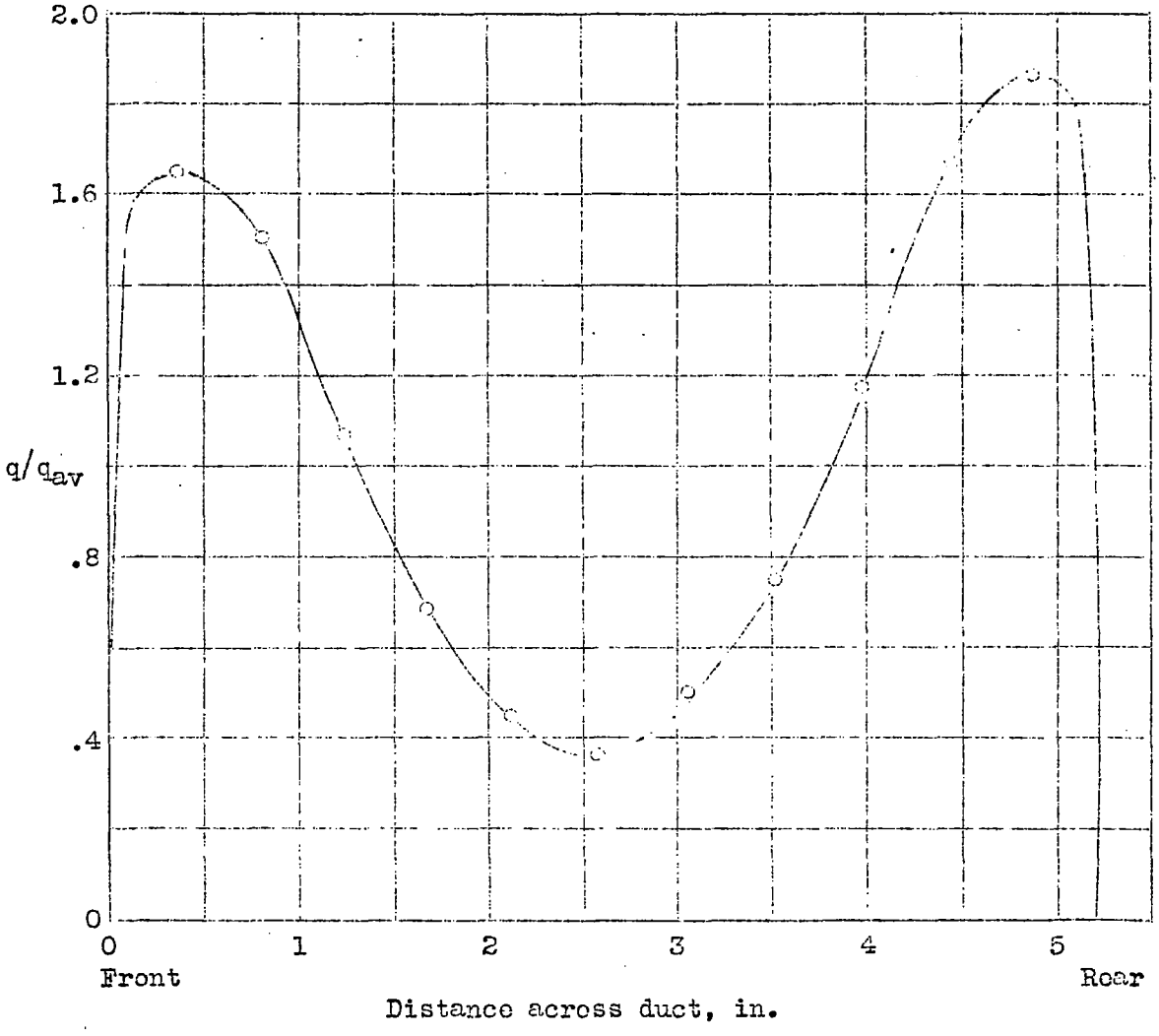

Figure 13.- Dynamic-pressure distribution in front of the carburetor and increment of metering pressure. $\Delta(A-B)$ = 3.5 percent.

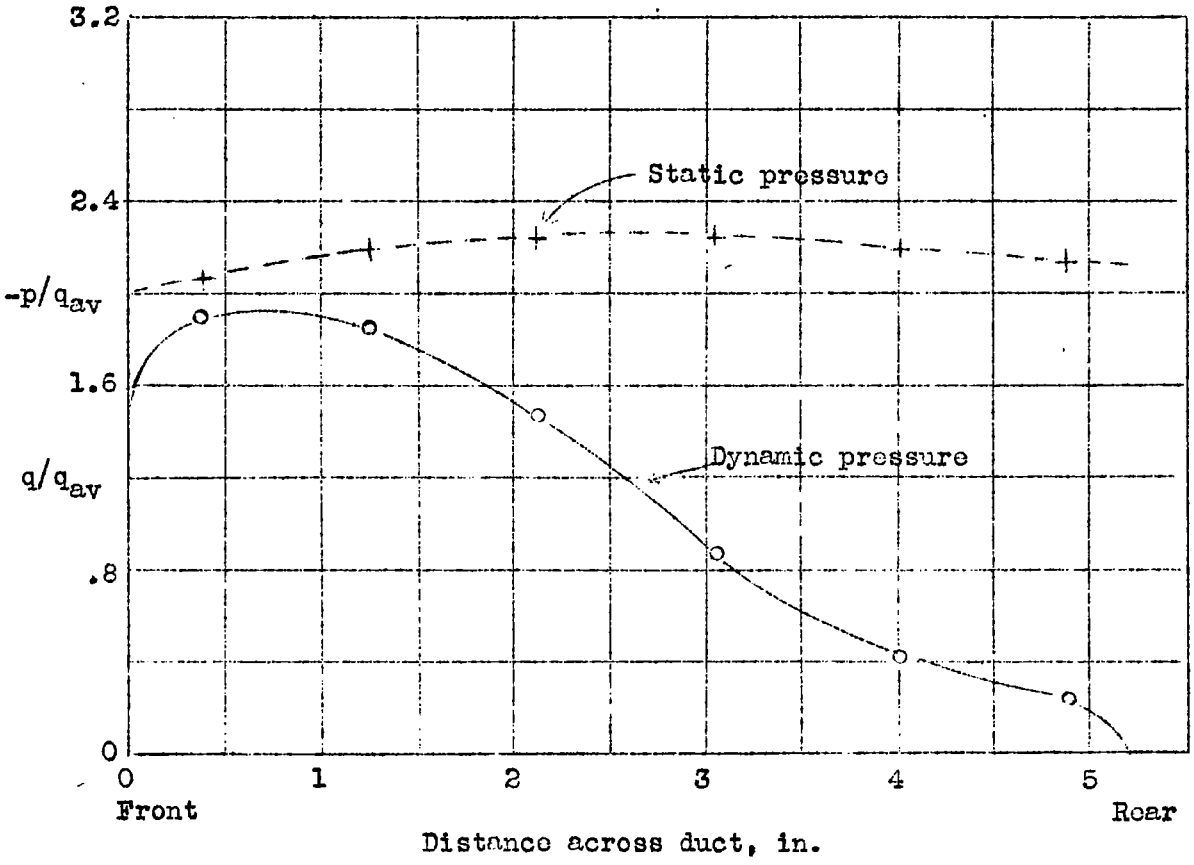

Figure 14.- Dynamic- and static-pressure distributions and increment of metering pressure with square elbow, 19 inches from carburetor. $\Delta(A-B)$ = 10.5 percent.

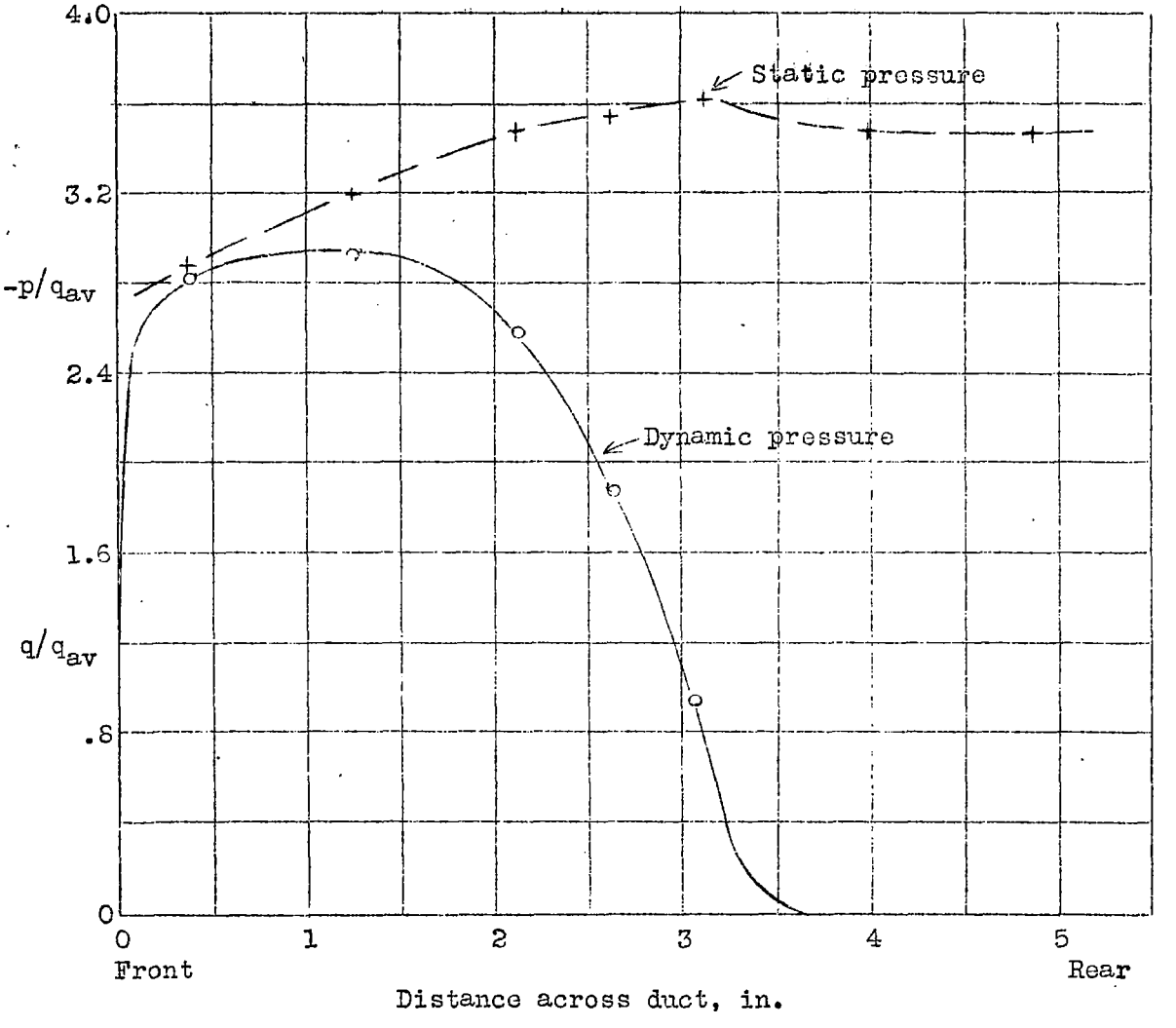

Figure 15.- Dynamic- and static-pressure distributions and increment of metering pressure with square elbow, 12 inches from carburetor. $\Delta(A-B) = 10$ percent; $(A-B)/\Delta p_v = 2.85$.

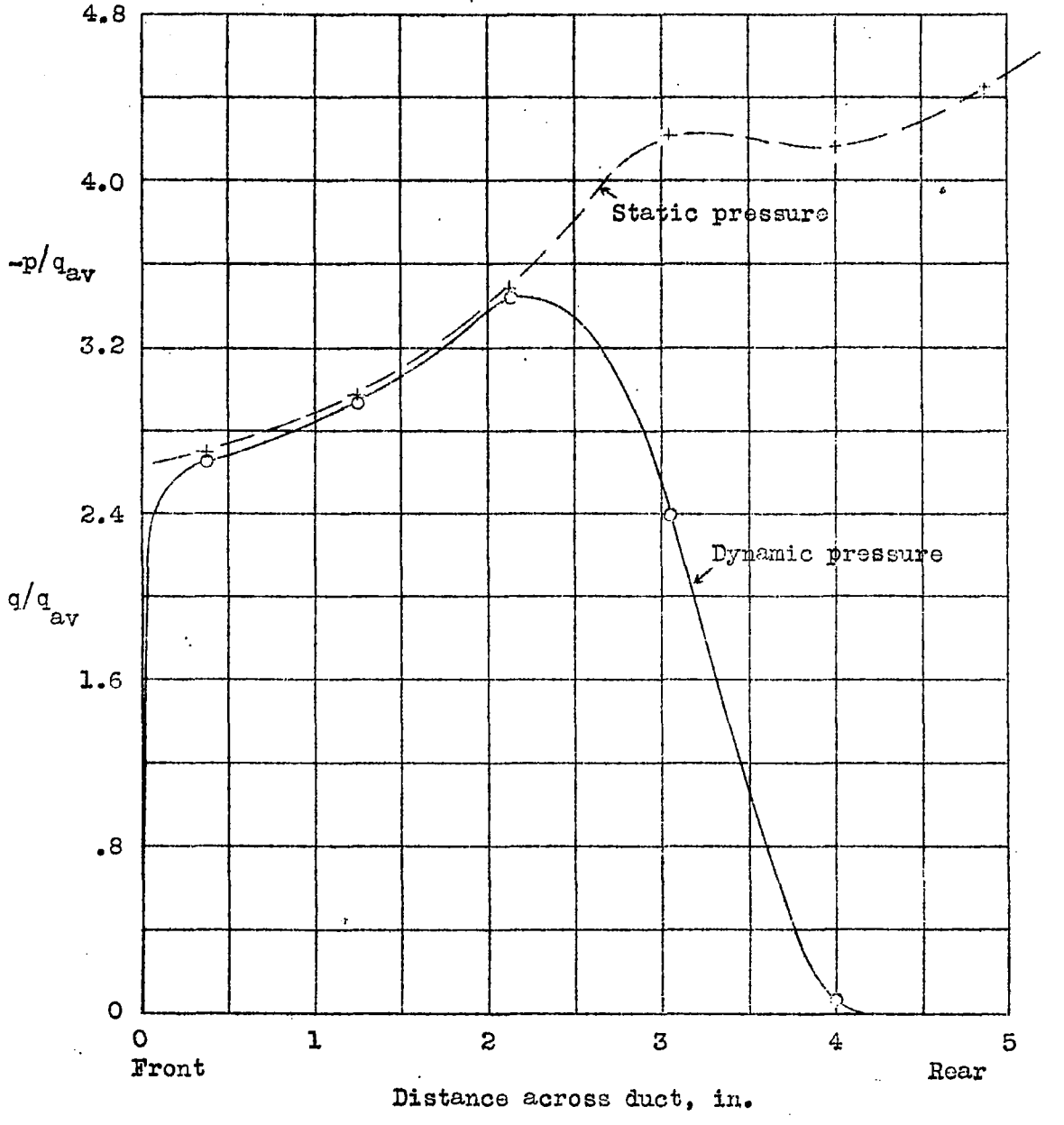

Figure 16.- Dynamic- and static-pressure distributions and increment of metering pressure with square elbow, 8 inches from carburetor. $\Delta(A-B)$ = 10 percent; $(A-B)/\Delta p_v$ = 2.97.

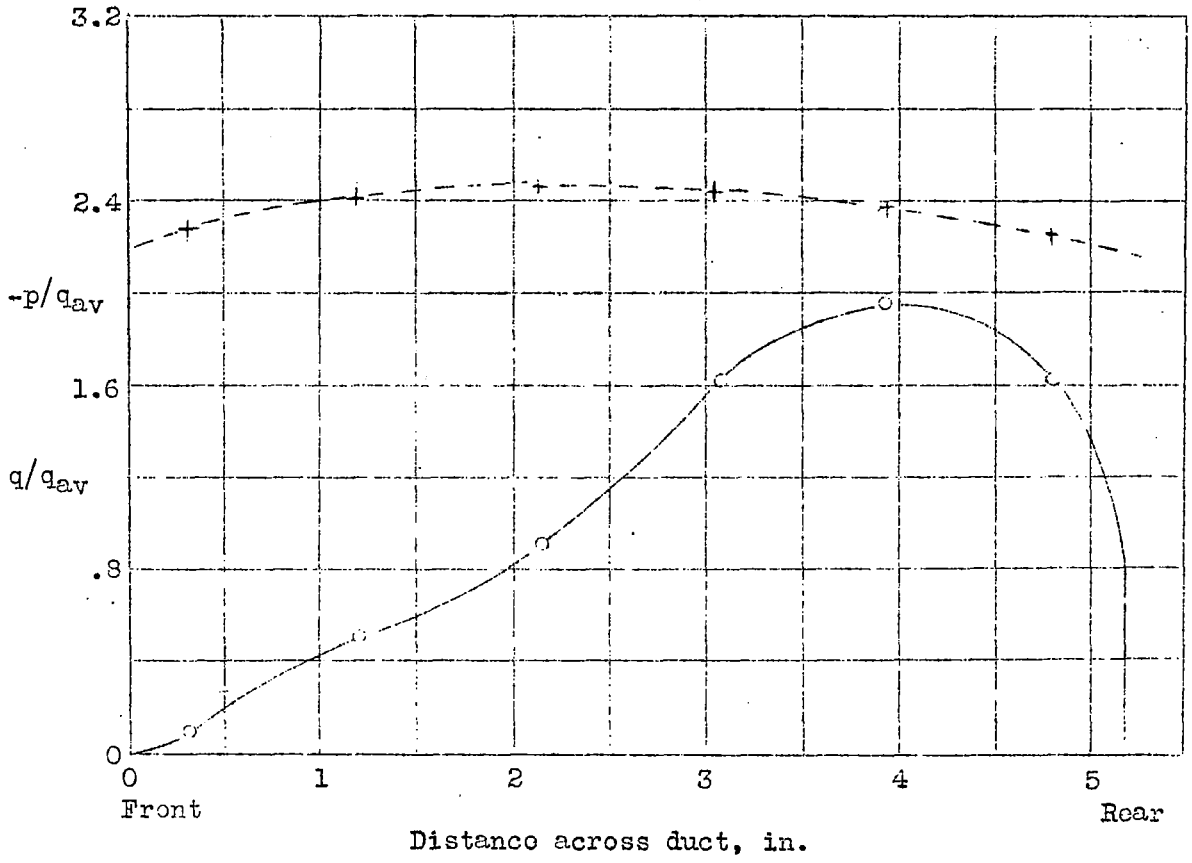

Figure 17.- Dynamic-and static-pressure distributions and increment of metering pressure with square elbow, 19 inches from carburetor. $\Delta(A-B)$ = 10 percent; $(A-B)/\Delta p_V$ = 2.72.

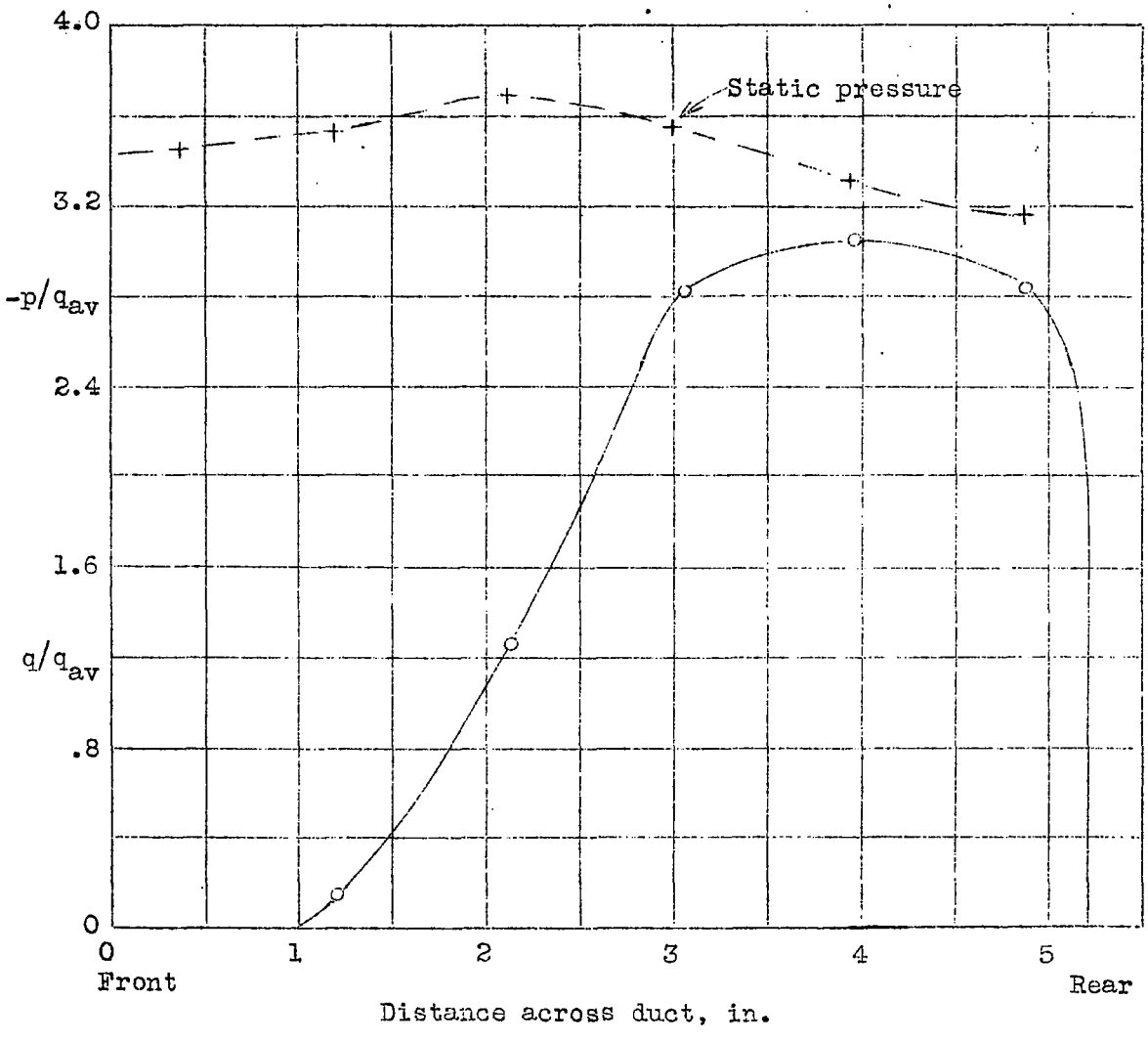

Figure 18.- Dynamic- and static-pressure distributions and increment of metering pressure with square elbow, 12 inches from carburetor. $\Delta(A-B) = 10$ percent; $(A-B)/\Delta p_v = 2.85$.

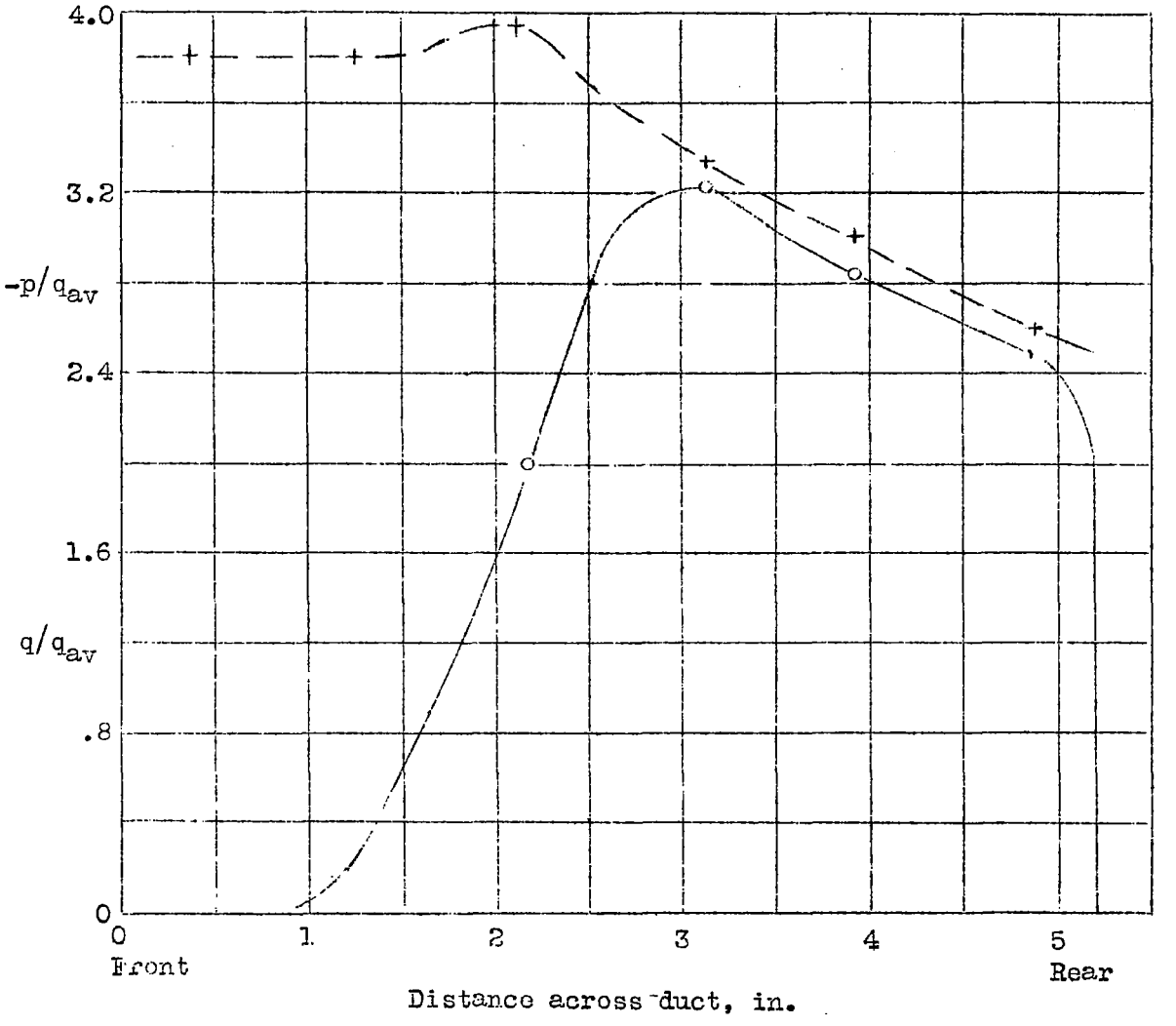

Figure 19.- Dynamic- and static-pressure distributions and increment of metering pressure with square elbow, 8 inches from carburetor. $\Delta(A-B) = 6.5$ percent; $(A-B)/\Delta p_v = 2.79$.

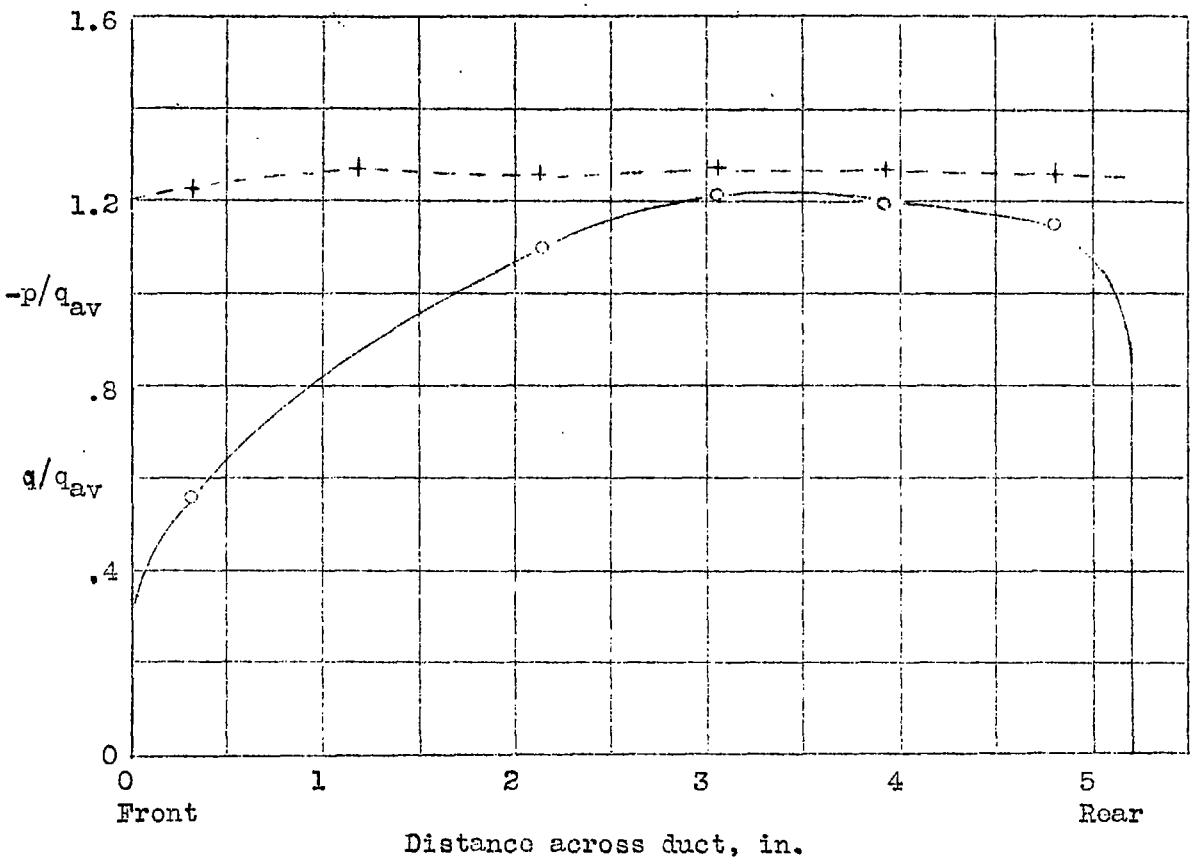

Figure 20.- Dynamic- and static-pressure distributions and increment of metering pressure with round elbow, 15 inches from carburetor. $\Delta(A-B) = 3$ percent; $(A-B)/\Delta p_v = 2.65$.

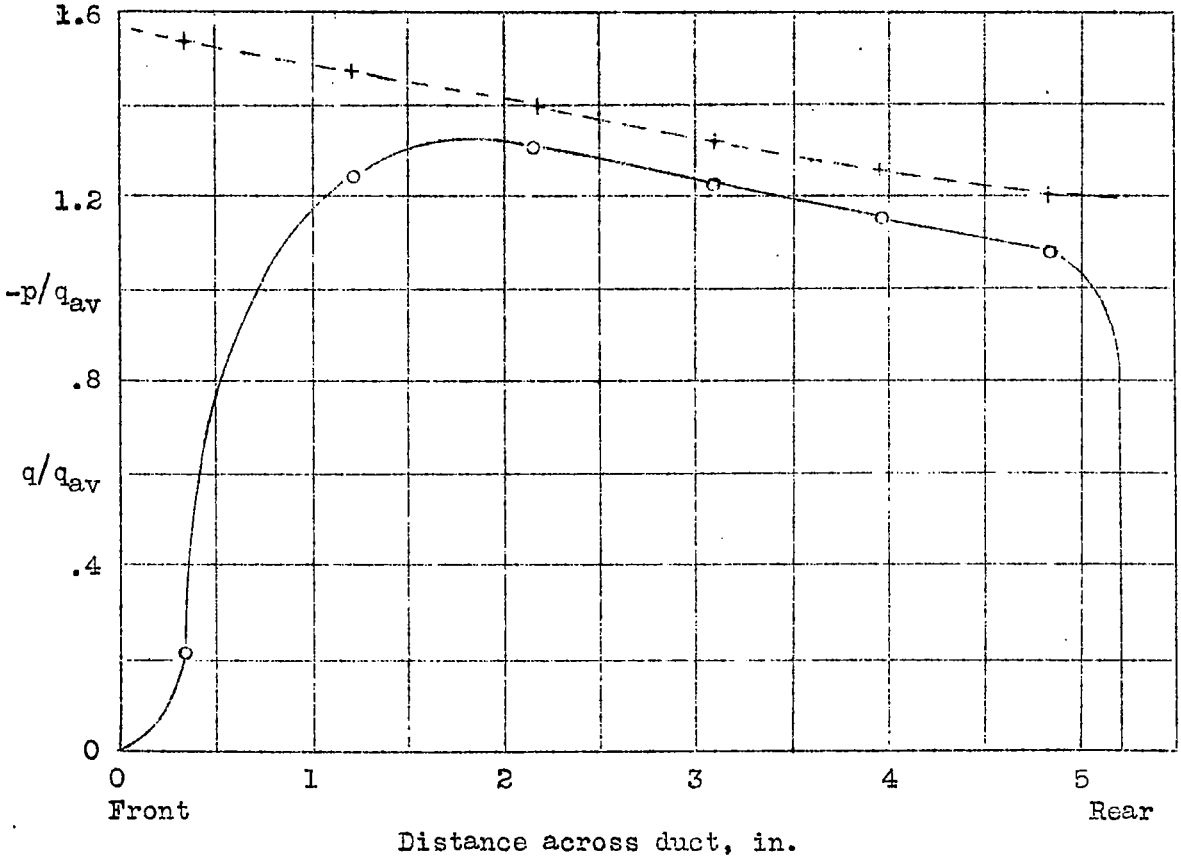

Figure 21.- Dynamic- and static-pressure distributions and increment of metering pressure with round elbow, 8 inches from carburetor. $\Delta(A-B) = 1.5$ percent; $(A-B)/\Delta p_v = 2.61$.

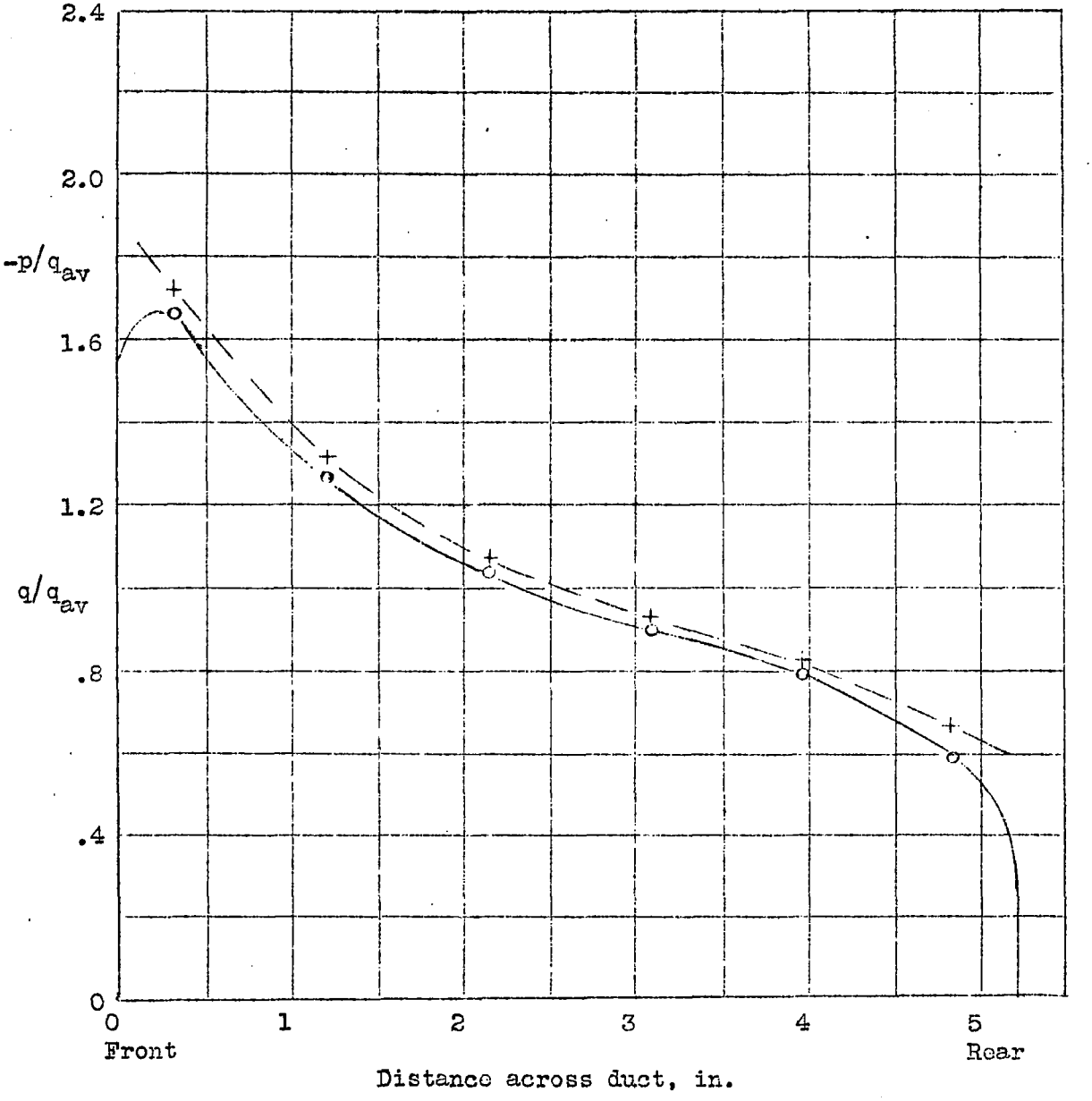

Figure 22.- Dynamic- and static-pressure distributions and increment of metering pressure with round elbow, 4 inches from carburetor. $\Delta(A-B) = 0$ percent; $(A-B)/\Delta p_v = 2.61$.

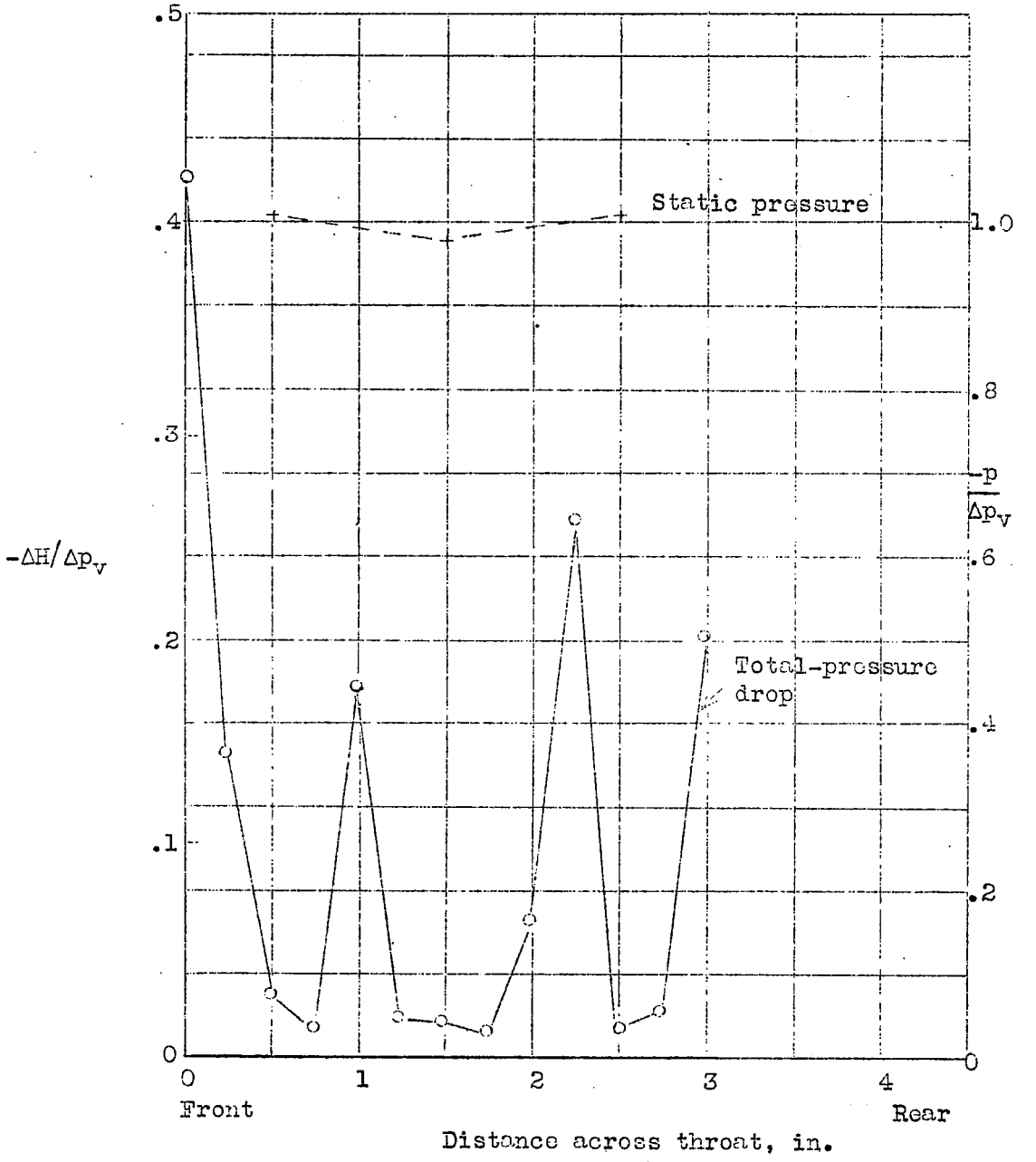

Figure 23.- Pressure measurements in the throat of the main venturi.

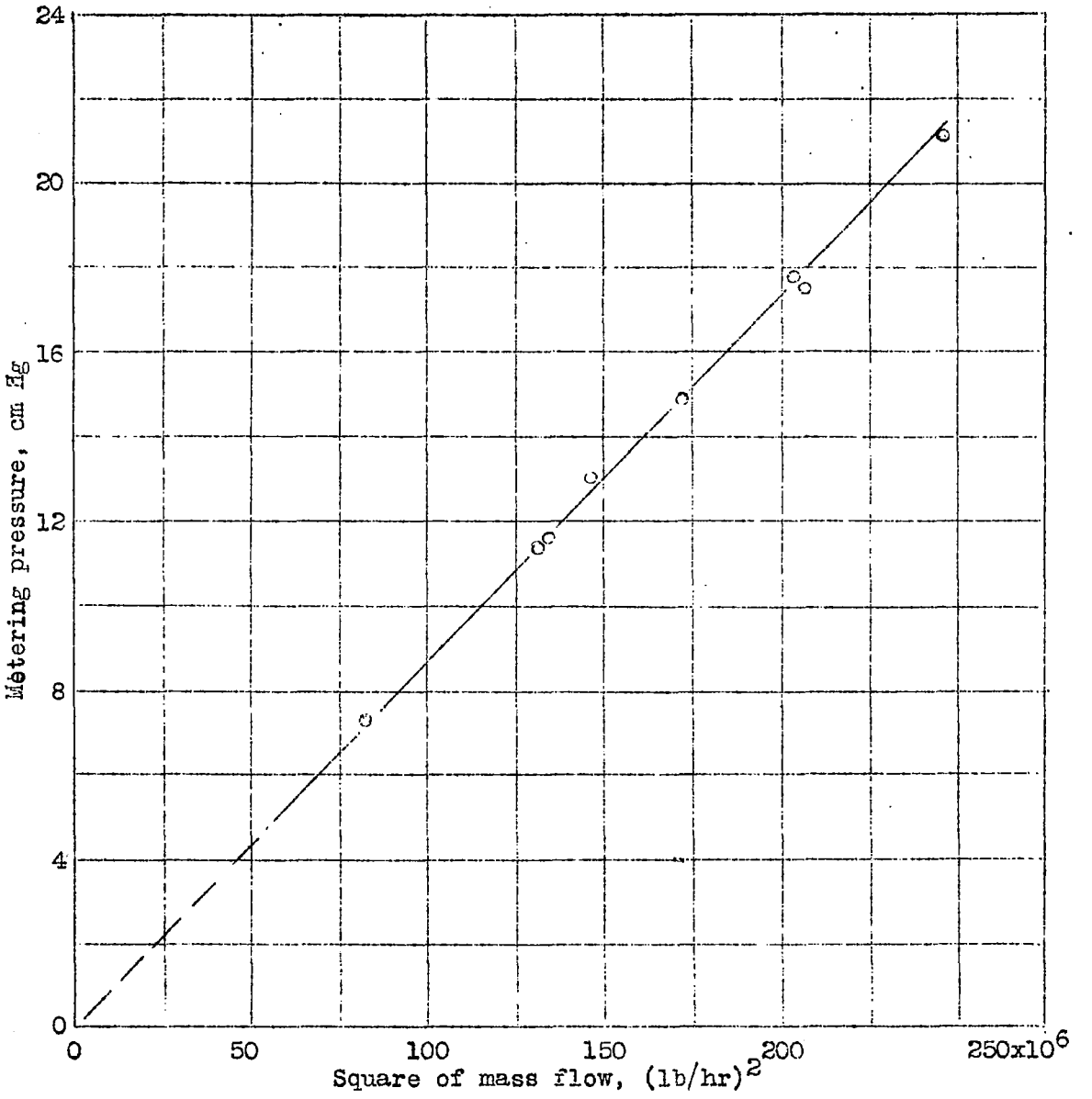

Figure 24.- Carburetor metering characteristics with uniform pressure distribution ahead of carburetor, automatic rich; $\rho = 0.00224$.

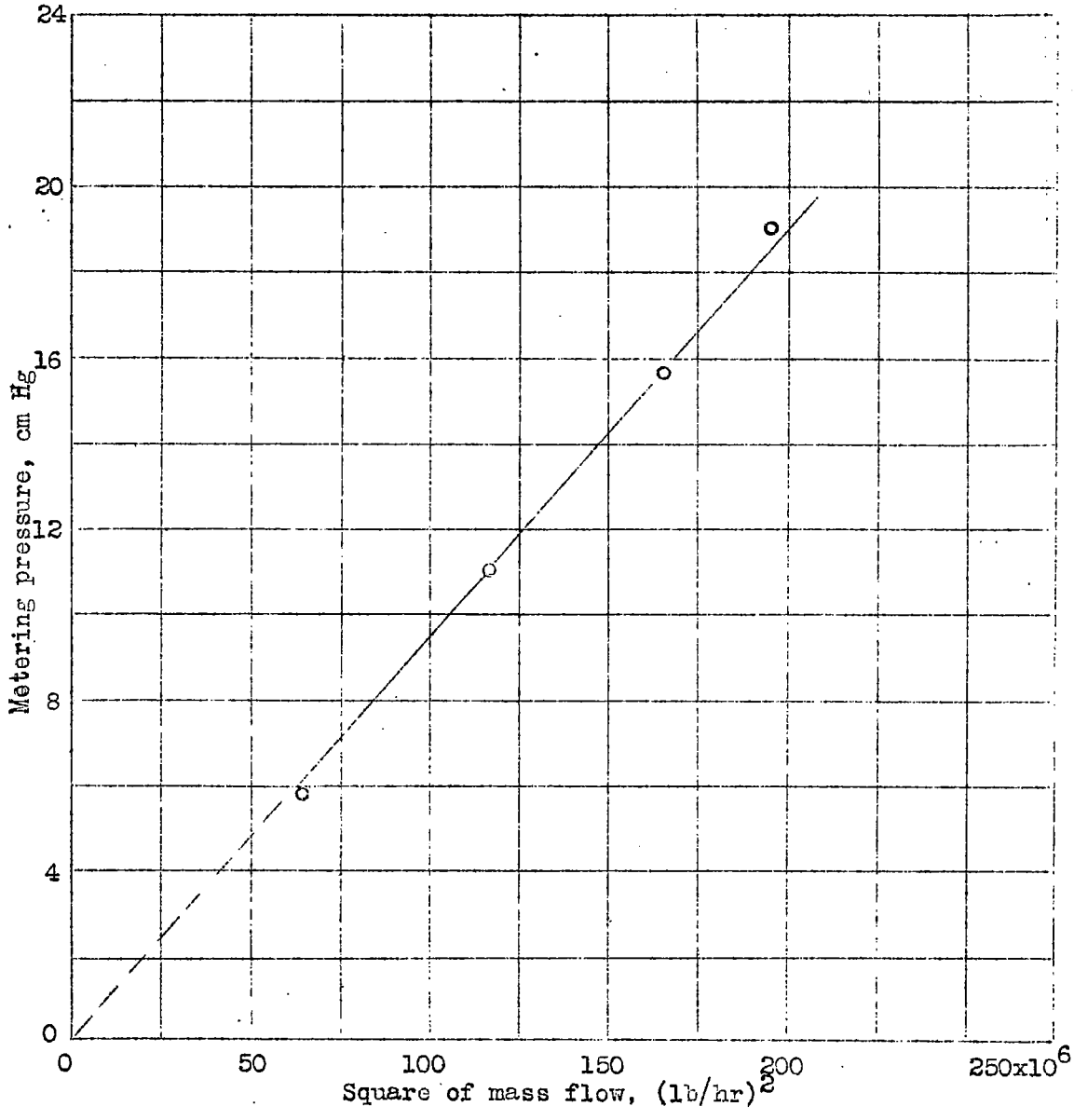

Figure 25.- Carburetor metering characteristics with uniform pressure distribution ahead of carburetor, emergency rich; $\rho = 0.00224$.

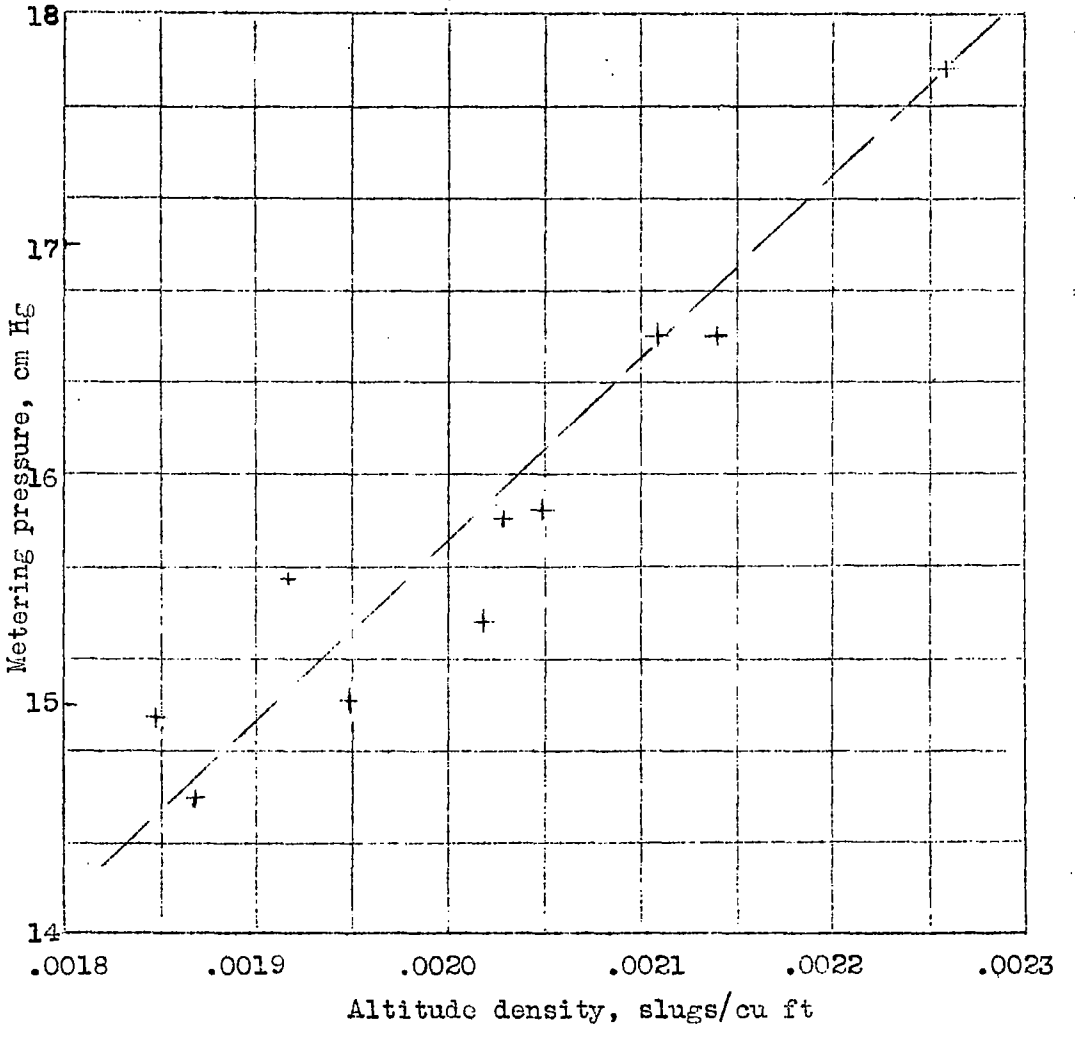

Figure 26.- Variation of metering pressure with altitude with same dynamic pressure in duct.